A Study of the Winston Red: The Smithsonian's New Fancy Red Diamond

Gabriela A. Farfan, Ulrika F.S. D'Haenens-Johansson, Stephanie Persaud, Eloïse Gaillou, Russell C. Feather II, W. Henry Towbin, and Daniel C. Jones

Red diamonds are among the rarest gems on Earth, especially Fancy red diamonds that are pure red and unmodified by brown, orange, or purple. At 2.33 ct, the Winston Red diamond is the fifth-largest Fancy red diamond known to exist and the only Fancy red diamond on public exhibit. On April 1, 2025, it was unveiled in a new exhibit at the Smithsonian National Museum of Natural History in Washington, DC. This is the first scientific and historical study conducted on this noteworthy stone. Optical observation along with spectroscopic, cathodoluminescence, and photoluminescence analyses confirmed the presence of plastic deformation bands and dislocation network patterns that classify the Winston Red as a type IaAB (A<B) Group 1 "pink" diamond and indicate that it underwent significant pressure and temperature conditions. The Winston Red owes its pure crimson color to a careful balance of absorption features: the 550 nm band associated with plastic deformation as well as the nitrogen-related N3 (N_3V^0), H3 (N_2V^0), and H4 ($N_4V_2^0$) defects. To place it in a broader context, the Winston Red's characteristics were compared to those of all other Fancy red diamonds that have been submitted to GIA. The history of the Winston Red diamond can now be traced back to 1938, but its old mine brilliant cut suggests an even richer story. Based on its mineralogical characteristics and history, the likely geographic origin of the stone has been narrowed down to Venezuela or Brazil; however, its precise origin remains unknown.

The 2.33 ct Winston Red diamond (figure 1) is on the verge of becoming one of the most famous fancy-color diamonds in the world. Currently the largest pure red diamond on public display, it is the fifth-largest red diamond with the coveted Fancy red GIA color grade. As part of one of the most significant donations to the National Gem Collection in the last decade, this diamond is the "cherry on top" of a world-class collection of fancy-color diamonds that went on display in an exhibit titled "The Winston Red Diamond and the Winston Fancy Color Diamond Collection" at the Smithsonian National Museum of Natural History (NMNH) on April 1, 2025.

Formerly referred to as the "Raj Red," the Winston Red is an old mine brilliant-cut diamond measuring approximately 8 mm in diameter with a very large culet and an extremely thin bruted girdle (again, see figure 1). The red color distribution is described as even, and the clarity is graded I_2 due to a combination of inclusions, chips around the girdle, and a particularly large but shallow feather that runs perpendicular to the table, as illustrated in the natural colored diamond report issued by GIA in 2023 (figure 2). Yet the color makes the Winston Red truly remarkable and one of the most beautiful red diamonds in the world.

In this study, scientists from the Smithsonian NMNH Department of Mineral Sciences teamed up with GIA and the curator from the Paris School of Mines to examine this rare diamond. This provided a unique opportunity to showcase the science behind the beautiful red color, interrogate the geological nature of its uncommon occurrence, and reveal the rich history of the stone before going on display at the Smithsonian. This investigation also highlights the threefold mission of natural history museums: to display awe-inspiring specimens, preserve natural history for future generations, and uncover new knowledge through scientific examination. Every specimen is

See end of article for About the Authors and Acknowledgments.
Gems & Gemology, Vol. 61, No. 1, pp. 16–42,
http://dx.doi.org/10.5741/GEMS.61.1.16
© 2025 Gemological Institute of America

Figure 1. The 2.33 ct Winston Red diamond, displaying a vibrant Fancy red color. The old mine brilliant-cut stone measures approximately 8 mm in diameter. Photo by Robert Weldon; courtesy of Ronald Winston.

useful for study—especially those that are extraordinary and historically valuable, such as the Winston Red diamond.

Comparison to Other Red Diamonds. Unmodified Fancy red diamonds are among the rarest objects of natural history on the planet; only 24 stones over one

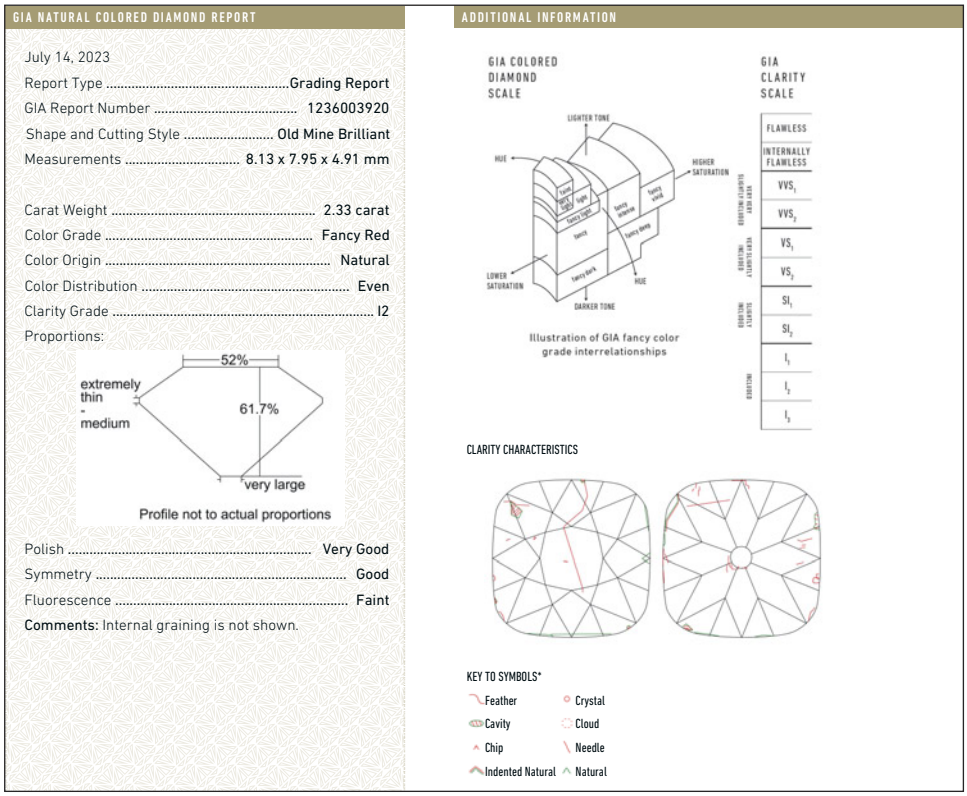

GIA NATURAL COLORED DIAMOND REPORT

July 14, 2023
Report Type ..... Grading Report
GIA Report Number 1236003920
Shape and Cutting Style ..... Old Mine Brilliant
Measurements ..... 8.13 x 7.95 x 4.91 mm

Carat Weight ..... 2.33 carat
Color Grade ..... Fancy Red
Color Origin ..... Natural
Color Distribution ..... Even
Clarity Grade I2
Proportions:

Profile not to actual proportions

Polish ..... Very Good
Symmetry ..... Good
Fluorescence ..... Faint
Comments: Internal graining is not shown.

ADDITIONAL INFORMATION

Illustration of GIA fancy color grade interrelationships

CLARITY CHARACTERISTICS

KEY TO SYMBOLS*

Feather, Crystal, Cavity, Cloud, Chip, Needle, Indented Natural, Natural

Figure 2. GIA Natural Colored Diamond Report for the Winston Red.

TABLE 1. Diamonds given a Fancy red (unmodified) color grade by GIA that are over one carat and reported in public records (e.g., auction and tender websites, publications), ranked by size.

Rank	Name	Weight (ct)	Cut or shape[a]	Clarity	Origin	References
1	Moussaieff Red	5.11	Trilliant	Unknown	Brazil, Minas Gerais, Rio Abaeté	King and Shigley, 2003; Wilson, 2014; Hoover et al., 2018
2	Winston Red	2.33	Old mine brilliant	I_2	Unknown	This study
3	Argyle Everglow	2.11	Cut-cornered rectangular modified brilliant	VS_2	Australia, Argyle	Argyle Tender, 2017
4	Unnamed	2.09	Heart brilliant	SI_2	Unknown	Christie's Hong Kong, 2014
5	Unnamed	1.92	Cut-cornered rectangular mixed cut	VS_2	Unknown	Phillips de Pury, New York, 2001; Sotheby's Hong Kong, 2011; Christie's Geneva, 2013
6	Argyle Enigma	1.75	Cut-cornered rectangular mixed cut	SI_2	Australia, Argyle	Argyle Tender, 2019
7	Noor Red	1.71	Heart brilliant	SI_2	Unknown	Sotheby's New York, 2020
8	Giacampos Red	1.57	"Oval"	Unknown	Brazil, Minas Gerais, Santo Inácio River	Svisero et al., 2017; Hoover et al., 2018
9	Argyle Phoenix	1.56	Round brilliant	I_2	Australia, Argyle	Argyle Tender, 2013; Phillips Geneva, 2024
10	Argyle Aurora	1.47	Oval modified brilliant	SI_2	Australia, Argyle	Argyle Tender, 2015
11	Unnamed	1.44	Cut-cornered rectangular mixed cut	I_2	Australia, Argyle	Sotheby's Geneva, 2022
12	Unnamed	1.38	Cushion modified brilliant	SI_2	Unknown	Sotheby's New York, 2019
13	Argyle Cardinal	1.21	Cut-cornered rectangular mixed cut	SI_2	Australia, Argyle	Argyle Tender, 2014
14	Red Miracle	1.21	Cut-cornered rectangular mixed cut	SI_2	Unknown	Phillips Geneva, 2024
15	Argyle Prima	1.20	Pear brilliant	SI_1	Australia, Argyle	Argyle Tender, 2015
16	Argyle Isla	1.14	Cut-cornered rectangular modified brilliant	I_1	Australia, Argyle	Argyle Tender, 2017
17	Argyle Mira	1.12	Cut-cornered rectangular modified brilliant	SI_2	Australia, Argyle	Argyle Tender, 2018
18	Argyle Scarlett	1.10	Oval brilliant	I_1	Australia, Argyle	Argyle Tender, 2009
19	Argyle Aria	1.09	Oval modified brilliant	I_1	Australia, Argyle	Argyle Tender, 2016
20	Argyle Avenoir	1.07	Oval modified brilliant	I_2	Australia, Argyle	Argyle Tender, 2019
21	Unnamed	1.06	Round-cornered rectangular modified brilliant	I_2	Unknown	Sotheby's Hong Kong, 2022
22	Unnamed	1.05	"Oval"	SI_2	Unknown	Christie's, 2002
23	Unnamed	1.03	Cut-cornered rectangular step cut	SI_1	Unknown	Sotheby's New York, 2021
24	Argyle Bohème	1.01	Cut-cornered rectangular modified brilliant	I_2	Australia, Argyle	Argyle Tender, 2021

[a]*Diamond shapes in quotation marks indicate cases in which cut details are unknown.*

In Brief

- At 2.33 ct, the Winston Red diamond, now on display at the Smithsonian National Museum of Natural History in Washington, DC, is the fifth-largest confirmed Fancy red diamond with a pure, unmodified red color.
- Fancy red diamonds are exceedingly rare, accounting for only approximately 0.04% of fancy-color diamonds submitted to GIA.
- The Winston Red's color is the result of a combination of absorption features: the 550 nm band associated with plastic deformation as well as the nitrogen-related N3 (N_3V^0), H3 (N_2V^0), and H4 ($N_4V_2^0$) defects.
- Investigation into its rich history and gemological properties suggest that the Winston Red most likely originates from Brazil or Venezuela.

carat exist in the public record, as identified in auction catalogs and news articles by this study (table 1). Beyond those listed in table 1, there are additional privately owned stones that have passed through GIA and other gemological laboratories but are excluded from these detailed tables as they are not public knowledge. The Winston Red is notable for being the fifth-largest unmodified Fancy red diamond among all the Fancy reds graded by GIA, and the second-largest Fancy red diamond that is in the public record, as listed in table 1. It is also the largest Fancy red diamond on public display now that it is officially part of the National Gem and Mineral Collection. The immense value of diamonds with the coveted Fancy red color grade is exemplified by the 2024 sale of the 1.56 ct, I_2 clarity Argyle Phoenix, which simultaneously commanded the highest price ($4.2 million) and price per carat ($2.7 million/ct) for a Fancy red diamond to date.

More than 20 years ago, the largest confirmed Fancy red diamond, the 5.11 ct Moussaieff Red, was on loan for the temporary "Splendor of Diamonds" exhibit at the Smithsonian NMNH in 2003 (King and Shigley, 2003). Since then, the only red-hued diamond exhibited at the Smithsonian has been the 5.03 ct DeYoung Red, with a darker, "red-brown" color (table 2; Shigley and Fritsch, 1993). Notably, in GIA's color grading system, a diamond is not considered a red diamond unless the final word in the color description is *red*. Hence some historically "red" diamonds listed in table 2 may include stones that were not predominantly red, such as the DeYoung Red. The stark differences in hue and saturation between the Winston Red and the DeYoung Red are visible when they are placed side by side (figure 3).

In 1987, GIA examined the Winston Red and issued a gem identification report describing it as a "brownish-orange-red" diamond. The fancy-color grading system has since been refined and standardized with controlled viewing and lighting environments, expanded terminology, and color comparators such as colored diamond master stones and Munsell color chips (King et al., 1994). King et al. (2002) highlight the particular challenge of color grading predominantly red diamonds. Their scarcity left few historic points of reference, resulting in a range of opinions regarding what a "red" diamond should look like. A Fancy red diamond has a unique appearance compared to other red gemstones. The GIA Natural Colored Diamond Report issued in 2023, with modern color grading, determined that the Winston Red is Fancy red (again, see figure 2).

Natural, untreated diamonds that have been described by GIA as having a predominantly red hue are exceedingly rare (e.g., Kane, 1987; King et al., 2002, 2014; King and Shigley, 2003; Eaton-Magaña et al., 2018). Analysis of more than a million natural fancy-color diamonds submitted to GIA for laboratory

Figure 3. The Winston Red diamond (center, 2.33 ct), alongside the much darker "red-brown" DeYoung Red (left, 5.03 ct) and the DeYoung Pink diamonds (right, 2.82 ct). All three stones are currently on public exhibit at the Smithsonian NMNH. Photo by Gabriela Farfan.

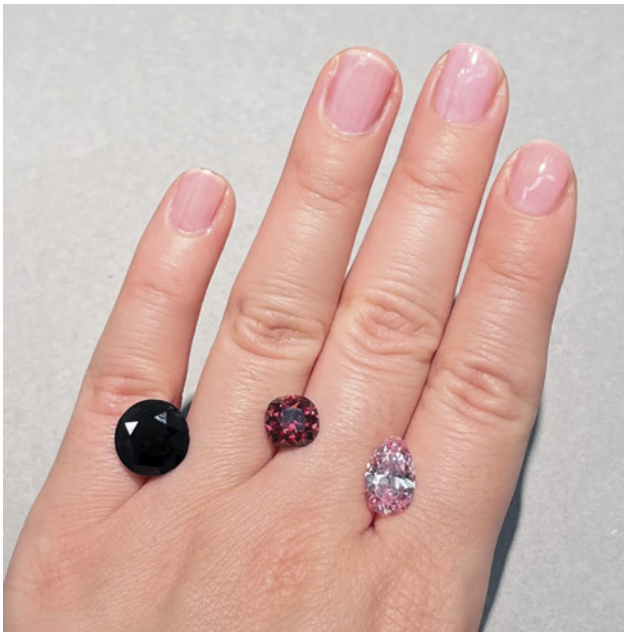

TABLE 2. Significant "red" diamonds described as reddish or red in the public domain of sizes larger than the 2.33 ct Winston Red diamond.

Rank[a]	Name	Weight (ct)	Shape	Color description or color grade[b]	Notes	References
Unconfirmed	Lichtenburg Red	18	Rough	"Red"	—	Wilson, 2014
Unconfirmed	Unnamed	10.26	Pear	"Chinese red"	—	Wilhelm, 1860, pp. 126–127; Shigley and Fritsch, 1993
Unconfirmed	Unnamed	8.00	Unknown	"Red"	—	Shigley and Fritsch, 1993; Kunz, 1926, p. 596
Unconfirmed	Unnamed	7.44	Round	"Garnet"	—	Wilhelm, 1860, pp. 108–109; Shigley and Fritsch, 1993
Unconfirmed	Unnamed	6.00	Cushion	"Red"	Reportedly from South Africa	Kunz, 1926, p. 596; Gill, 1978, p. 85; Shigley and Fritsch, 1993
Unconfirmed	Edcora Red	5.71	Pear	"Red-brown"	Called the "lost stone"; last seen in Hong Kong	—
1	Moussaieff Red	5.11	Triangular	Fancy red	Formerly "Red Shield"	King et al., 2002; King and Shigley, 2003
2	Kazanjian Red	5.05	Square	"Blood red"	Formerly "De Beers Red"; reportedly from Lichtenburg, South Africa	Drukker, 1971; Gaal, 1977, p. 241; Gill, 1978, p. 85; Shigley and Fritsch, 1993
3	DeYoung Red	5.03	Round	"Red-brown"	—	Shigley and Fritsch, 1993
4	Unnamed	5	Unknown	"Ruby red"	—	Shepherd, 1934; Monnickendam, 1955, p. 154; Shigley and Fritsch, 1993
5	Unnamed	5	Round	"Port wine red"	—	Gill, 1978, p. 86; Shigley and Fritsch, 1993
6	Unnamed	3.98	Round	"Brownish red"	—	Wilhelm, 1860, pp. 94–95; Shigley and Fritsch, 1993
7	Fancoldi Red	3.16	Round	Fancy Intense purplish red	—	Wilson, 2014; Hoover et al., 2018
8	Christmas Red	3.15	Round	Fancy reddish orange	—	Wilson, 2014
9	Unnamed	2.50	Round	"Port wine red"	—	Gill, 1978, p. 86; Shigley and Fritsch, 1993
10	Unnamed	2.50	Marquise	"Deep cherry red"	—	Gill, 1978, p. 86; Shigley and Fritsch, 1993
11	Unnamed	2.50	Round	"Red"	Reportedly from Brazil	Gill, 1978, p. 85; Shigley and Fritsch, 1993
12	Winston Red	2.33	Cushion[c]	Fancy red	Formerly "Raj Red"	—

[a]The first six are not ranked as their records cannot be confirmed.
[b]Color descriptions in quotation marks indicate cases in which formal fancy-color grades are not available.
[c]Shape refers to a cut diamond's outline; hence the old mine brilliant-cut Winston Red diamond has a cushion shape.

services (i.e., excluding D-to-Z color diamonds) reveals that predominantly red diamonds account for only approximately 0.07% of the stones. Among these red diamonds, those graded Fancy red account for 56.9% (i.e., 0.04% of all fancy-color diamonds), with the remainder modified by purple (39.5%), orange (2.0%), or brown (1.6%). King et al. (2002) describe and illustrate the differences between the Fancy Deep pink, Fancy Vivid pink, and Fancy red color grades, noting the distinctive tone and saturation associated with Fancy red diamonds. The narrow ranges of tone and saturation for diamonds described as red also mean that they can receive only one fancy grade: Fancy. The only other colors that warrant this approach are Fancy black and Fancy white diamonds.

The geological processes involved in creating red color in diamonds are extreme (discussed later) and may contribute to the small sizes and lower clarity grades that most red diamonds have received from GIA (see appendix 1 at https://www.gia.edu/gems-gemology/spring-2025-winston-red-diamond). The vast majority of Fancy red (i.e., unmodified) diamonds are small, with only 4% larger than two carats, the largest being the 5.11 ct Moussaieff Red. Over 75% of Fancy red diamonds have received clarity grades of SI_1 to I_2, and approximately 30% have I_1 or I_2 clarity grades. In order of incidence, the most common clarity features were feathers, crystal inclusions, and natural surfaces. For most buyers, lower clarity in Fancy red diamonds is of little concern compared to the coveted red color (King et al., 2014). Typically, the shapes and cutting styles for Fancy red diamonds were chosen to maximize weight and enhance face-up color, with less than 4% of diamonds being cut into round shapes. The three most common shapes were rectangular (50%), square (16%), and oval (12%). Popular cutting styles were modified brilliants, most notably the cut-cornered rectangular and square modified brilliants, referred to as "radiant cut" in the trade.

The Winston Red ranks 12th in size among the larger confirmed "red" diamonds of the world, according to public records (table 2). The largest confirmed historically "red" diamonds are the Moussaieff Red (5.11 ct trilliant cut), followed by the Kazanjian Red (5.05 ct square cut), and the DeYoung Red (5.03 ct round brilliant cut). Still, accounts of six even larger reddish diamonds (18, 10.26, 8.00, 7.44, 6.00, and 5.71 ct) have been listed in previous studies as recorded in the Gem Catalogue of the Duke of Brunswick-Luneburg in 1860 and others (Kunz, 1926; Gill, 1978; Shigley and Fritsch, 1993; Wilson, 2014). It is important to note that although table 2 encompasses diamonds historically regarded as red, most lack a formal color grade. Other than the Moussaieff Red and Winston Red, none of the significant red diamonds in table 2 have received the Fancy red color grade (indicating pure, unmodified red) that follows today's standards, and most are red with modifying colors (e.g., Fancy purplish red) or have not been graded by GIA. Some, such as the DeYoung Red, are described as red-brown and other colors that would not qualify as red today because the final word in the color description is not "red" (e.g., brownish red).

Categorizing Pink and Red Diamonds. It is well established that red diamonds acquire their color through the same mechanisms as pink diamonds (red is a more saturated pink color), relating to crystal deformation (King et al., 2002; Eaton-Magaña et al., 2018). In this article, we will discuss red and pink diamonds interchangeably. Here, we explore the literature on causes of color in pink and red diamonds to compare to the Winston Red and provide clues about its color origin, geological formation, and even geographic origin.

Although diamond is considered a hard, brittle material, it can deform plastically under applied pressures at high temperatures (Smith, 2023). Plastic deformation of diamond involves the generation of dislocations and their movement, generally resulting in slip along octahedral {111} planes in <110> directions (Evans and Wild, 1965). Diamond crystal distortion can also lead to an abrupt and localized change in the lattice orientation, resulting in mechanical twinning (Titkov et al., 2012). Following plastic deformation, natural annealing processes can also lead to dislocations reorganizing into lower-energy arrangements, notably the polygonized dislocation networks with cellular appearances observed in deformed low-nitrogen diamonds (e.g., Sumida and Lang, 1981; Kanda et al., 2005; Fisher, 2009; Laidlaw et al., 2021). Pink diamonds are often separated into groups that consider the nitrogen content as defined by the diamond type classification system (described by Breeding and Shigley, 2009), as well as the distribution of the pink color. This naming convention was originally developed by Gaillou et al. (2010, 2012) and expanded by Eaton-Magaña et al. (2020). Briefly, Group 1 pink diamonds are defined as those containing low concentrations of aggregated nitrogen, with B-centers (N_4V^0) dominating over A-centers (nitrogen pairs) (type IaA<B). Microscopic observations show pink color throughout the stones, with wavy lamellae or graining. Detailed analyses through luminescence

imaging techniques reveal cellular dislocation patterns, typical of plastically deformed diamonds with low nitrogen. In contrast, Group 2 pink diamonds are type IaA>B with higher nitrogen concentrations. Their pink color is restricted to straight, discrete pink lamellae attributed to mechanical microtwinning, with colorless regions between the lamellae. Glide planes coinciding with the lamellae can be observed by luminescence imaging. The relative concentrations of A- and B-centers are often used to separate Group 1 and Group 2 pink diamonds, frequently stated as Group 1 = IaA<B, Group 2 = IaA>B. However, expanded Fourier-transform infrared (FTIR) analysis of pink diamonds suggests that Group 1 diamonds are characterized by %IaB>35% (Howell et al., 2015). Finally, Group 3 diamonds are comparatively "nitrogen-free" type IIa diamonds (detected by FTIR absorption), with uniform pink color created by the same crystallographic defects responsible for the pink color in Group 1 and Group 2 diamonds. In this study, we exclude the rare (light) pink type IIa diamonds colored by $NV^{0/-}$ centers (e.g., Eaton-Magaña et al., 2020), also called "Golconda pink diamonds," as the Winston Red diamond does not fall into that category.

HISTORY OF THE WINSTON RED

When the Winston Red diamond—formerly referred to as the "Raj Red"—first arrived at the Smithsonian, we knew very little about its history. The stone's donor, Ronald Winston, noted that he had purchased the stone from the Maharaja of Jamnagar from India in the late 1980s (R. Winston, pers. comm., 2023). Yet the stone's old mine cut promised a much richer history. Currently, we have traced the Winston Red's history back to September 1938, when Jacques Cartier sold the stone to the Maharaja of Nawanagar, Digvijaysinhji (also known as "the Good Maharaja"). In the Cartier London archives is a November 1938 communication to the maharaja in which Jacques Cartier wrote that he could envision the diamond set in a ring or "put in your big necklace between the green diamond and the pink diamond pendeloque […]. The red diamond would take the place of the white triangular diamond." There is no record of the red diamond being set by Cartier, and it was apparently sent to India shortly after the letter was sent. Unfortunately, at this time, Cartier archivists have not been able to uncover when or where Cartier acquired the diamond before

Figure 4. The Ceremonial Necklace of Nawanagar created by Cartier London and worn by the maharaja (A); originally sketched by Cartier in 1931, without the red diamond (B); and reproduced by A.V. Shinde circa 1958 and in 2002, containing a 2.34 ct red diamond (C). Photos courtesy of Archives Cartier Paris © Joshi & Vara, Archives Cartier London © Cartier, and Keswani (2004), respectively.

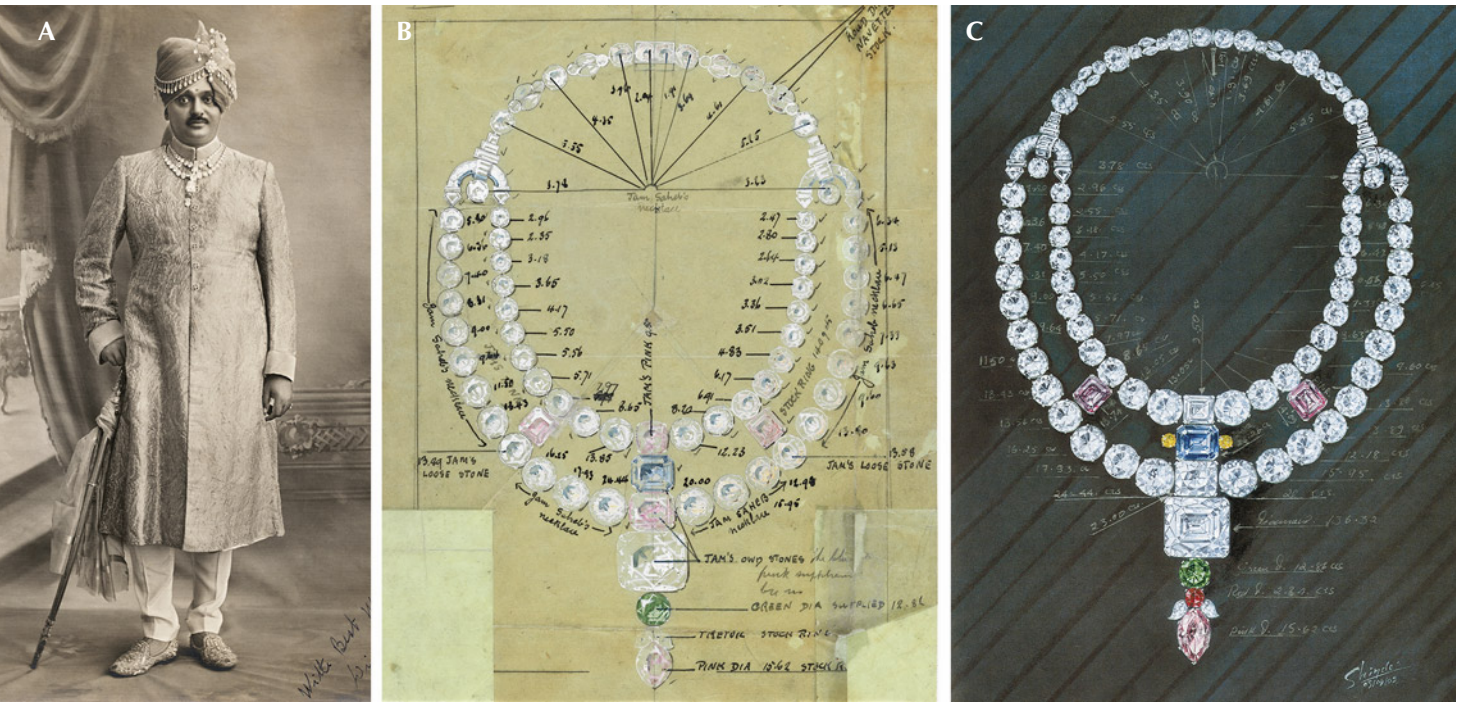

selling it to the maharaja. We are hopeful that more information will eventually provide additional clues about the stone's history and geographic origin.

The "big necklace" that Jacques Cartier referred to was the Ceremonial Necklace of Nawanagar, which Cartier assembled and considered one of his greatest works (figure 4, A and B, from the Cartier Archives; Spink, 2018; F. Cartier Brickell, pers. comm., 2024). This magnificent necklace contained over 600 carats of diamonds, including large pink, blue, and green stones highlighted by the 136.32 ct blue-white Ranjitsinhji diamond. It was commissioned in 1931 for the previous Maharaja of Nawanagar, Ranjitsinhji, who was Digvijaysinhji's uncle. In *The Biography of Colonel His Highness Shri Sir Ranjitsinhji Vibhaji* by Roland Wild, Jacques Cartier (1934) wrote a section in the appendix about the Nawanagar Jewels. He stated that the necklace was "the most extraordinary piece of the whole collection—a really superb realization of a connoisseur's dream." The version of the necklace with the red diamond added at the bottom was later re-sketched by A.V. Shinde circa 1958 and in 2002 (figure 4C).

In 1947, several newspapers showed evidence of the red diamond being set into the Ceremonial Necklace of Nawanagar, as Cartier originally suggested, in an image of the maharaja holding the necklace (figure 5). We currently do not know by whom or when it was set into the necklace. By the early 1960s, the necklace was being dismantled. Still, the Ceremonial Necklace of Nawanagar managed to maintain a certain level of fame beyond its lifetime. In 2018, it served as inspiration for the movie *Ocean's 8*, which features a copy of the necklace nicknamed the "Toussaint Necklace" after a former Cartier creative director, Jeanne Toussaint. Using only colorless diamonds (represented by cubic zirconia diamond imitations in the movie prop created by Cartier), the original design was modified to be smaller and worn by the actress Anne Hathaway.

In 1988, Ronald Winston, son of famous jeweler Harry Winston, acquired the red diamond from Digvijaysinhji's son Jam Saheb Sri Shatrusalyasinhji, who succeeded his father as the titular Maharaja of Nawanagar in 1966. The "Raj Red" diamond, as Winston called it at the time, was to be publicly unveiled at the November 1988 opening of the Harry Winston salon in Tokyo, but the festivities were postponed in deference to the failing health of Japan's Emperor Hirohito. Instead, the diamond debuted one year later at the anniversary of the Tokyo salon's opening, where actress Brooke Shields wore it mounted in a gold pinky ring (figure 6). She was also adorned in a white diamond necklace and a blue diamond ring, a trio that Winston touted as the "American Collection."

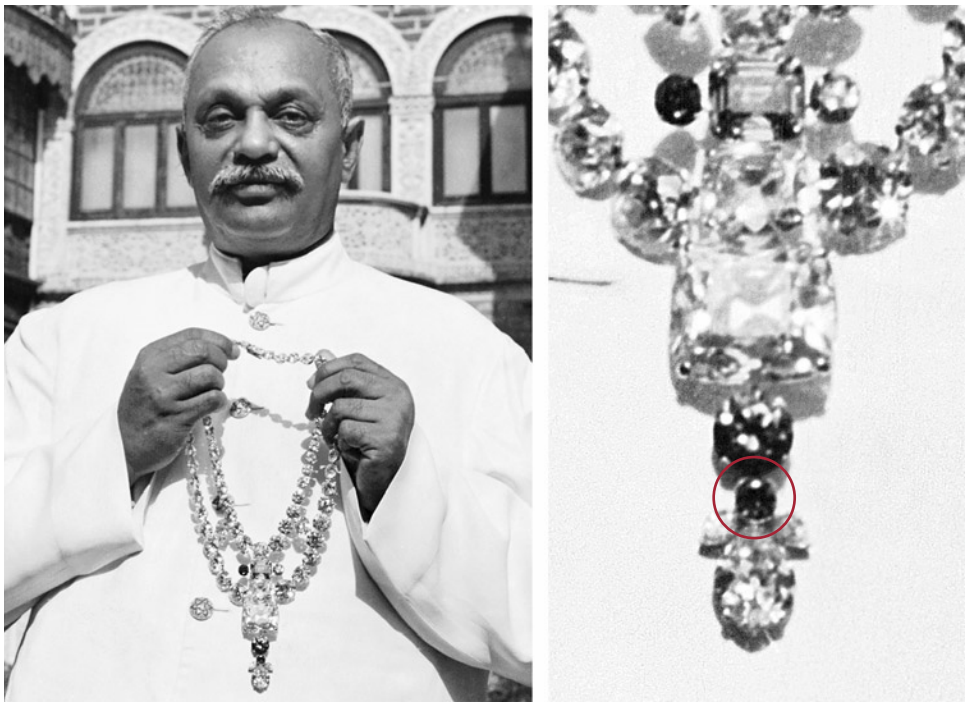

Figure 5. Left: The Ceremonial Necklace of Nawanagar held by the Maharaja Digvijaysinhji in 1947. Photo courtesy of Cartier Paris Documentation © Acme Photo. Right: Zoomed in on the red diamond, circled in red.

Figure 6. Brooke Shields wears the Winston Red diamond set in a pinky ring as part of the "American Collection" for a 1989 Harry Winston event in Tokyo. Photo by Itsuo Inouye; courtesy of Associated Press.

In December 2023, Ronald Winston officially gifted the diamond, now known as the Winston Red, to the National Gem Collection at the Smithsonian NMNH, where it resides in Washington, DC. The Winston Red is now on exhibit in the Winston Gallery as a neighbor to the Hope diamond, displayed alongside a subset of 40 stones from Winston's world-class collection of more than 100 other fancy-color diamonds.

METHODS

The Winston Red diamond was carefully studied using a range of spectroscopic and imaging techniques to gain a better understanding of the combination and distribution of point and extended defects responsible for its red color, providing insights into its formation and geological history. Combining forces, GIA scientists traveled to the NMNH with an instrument suite for diamond analysis and set up a temporary lab in the Department of Mineral Sciences to study the diamond using an expanded array of instruments from both organizations.

Optical Imaging. Photomicrographs were captured with a Nikon DS-Ri2 camera with a SMZ-2 microscope base with a 1× plan apo objective (1–11.25× magnification) under darkfield, brightfield, and fiber-optic illumination. Anomalous birefringence patterns, indicative of strain, were evaluated by placing the sample between cross-polarized filters under brightfield illumination.

FTIR Absorption Spectroscopy. A room-temperature FTIR absorption spectrum covering the 400–6000 cm^{-1} range with a 1 cm^{-1} resolution was collected using a Thermo Fisher Nicolet iS50 spectrometer equipped with a KBr and quartz beam splitters, a MCT-A detector, and a DRIFT (diffuse-reflectance infrared Fourier transform) accessory. The system and sample chamber were purged with dry air to minimize absorption features from atmospheric water. Unlike the other data of the Winston Red presented in this study, the FTIR spectrum used for defect concentration analysis was originally collected at GIA when it was submitted for grading in 2023.

Visible/Near-Infrared (Vis-NIR) Absorption Spectroscopy. An absorption spectrum spanning across the visible to near-infrared range (400–987 nm) was recorded with a custom-built GIA instrument using a fiber-coupled spectrometer (Ocean Optics QE Pro), a multicore reflection probe, and a tungsten-halogen light source (Avantes AvaLight-Hal-S-Mini). This high-resolution apparatus enabled the detection of very weak and sharp absorption features with the sample cooled to liquid nitrogen temperature (77 K).

Photoluminescence (PL) Spectroscopy. Photoluminescence spectroscopy analysis was carried out using three different instruments: two were non-confocal, collecting bulk emission spectra, whereas the third was a high-resolution confocal system used to map the distribution of luminescent defects. The first bulk-analysis instrument, designed and built by GIA, uses a 405 nm fiber-coupled laser (CNI FC-D-405-50mW) for excitation, with the room-temperature diamond placed on a small platform directly onto the output fiber. The PL signal was collected through a similarly positioned fiber and analyzed using a spectrometer with ~1.2 nm spectral resolution (Avantes Avaspec-Mini).

The second custom device allowed us to investigate the diamond's PL when cooled to 77 K using a wide selection of laser excitations. The sample was placed in a foam cup containing liquid nitrogen, and the excitation was delivered through direct contact with a bifurcated fiber coupled to a laser bank consisting of four Hübner Cobolt lasers: 457 nm (08-DPL 457 nm), 514.5 nm (06-MLD 514.5 nm), 633 nm (06-MLD 633 nm), and 830 nm (0.6-MLD 830 nm). The emission was collected and analyzed using a 550 mm Czerny-Turner spectrometer (Horiba iHR550) with a 600 l/mm grating and 90 µm slit width, leading to a spectral resolution of 0.13 nm using an EMCCD detector (Horiba Synapse EM).

Room-temperature PL maps were acquired using a Horiba Evolution Raman spectrometer equipped with 405 and 532 nm lasers, run with SwiftMode (set to 0.00001 sec/spot). Preliminary low spatial resolution maps over a selected pavilion facet were collected using a 5× objective (Olympus MPlan N, 0.1 NA) with the 405 nm laser (~5 mW) and a 300 l/mm grating over 412–522 nm. High spatial resolution maps (1× 1 µm steps and 0.25 × 0.25 µm steps) were then collected using a 50× long-distance objective (Olympus SLMPlan, 0.45 NA) and a 75 nm pinhole. Each map was collected with a 405 nm laser (~3 mW) to cover the 412–522 nm range and a 532 nm laser (~40 mW) to cover the 569–678 nm range. Where possible, PL maps were Raman normalized to account for slight sample tilt.

DiamondView Deep-UV Fluorescence Imaging. Fluorescence images under deep-UV illumination (<225 nm) were captured with a De Beers DiamondView system. Unlike standard short- and long-wave UV light sources, the above band-gap energy illumination provided by this device produces near-surface fluorescence from practically all diamonds. The resulting fluorescence images reveal clear patterns that can help decipher how a diamond grew and whether it was subjected to subsequent geological processes such as deformation (Welbourn et al., 1996; D'Haenens-Johansson et al., 2024). Different filters could be placed between the sample and the built-in camera; in addition to the standard filter that reduces signal contamination from the light source, colored filters were used to restrict the detected wavelengths: blue (390 nm band-pass), green (475 nm long-pass), orange (550 nm long-pass), and red (725 nm long-pass).

Scanning Electron Microscopy (SEM) and Cathodoluminescence (CL) Imaging. Cathodoluminescence and secondary electron images (SEI) were collected at the NMNH using a Thermo Fisher Quattro scanning electron microscope furnished with a retractable real color RGB CL detector (red, green, and blue channels). All analyses were collected using low vacuum mode at room temperature with 15 kV and 1.3 nA at a working distance of 10 mm. The Winston Red was uncoated for all of these measurements.

RESULTS AND DISCUSSION

Optical Microscopy. For orientation purposes, pavilion facet 1 (P1) is defined by a relatively large chip at the interface between P1 and the culet (figure 7A). The rest of the pavilion facets are labeled in clock-

Figure 7. Optical images of the Winston Red diamond. A: Chip between pavilion facet 1 (P1) and the culet. B: Labeled pavilion facets (P1–P8), as determined by the chip on P1. C: Graining viewed from P2. Photomicrographs by W. Henry Towbin.

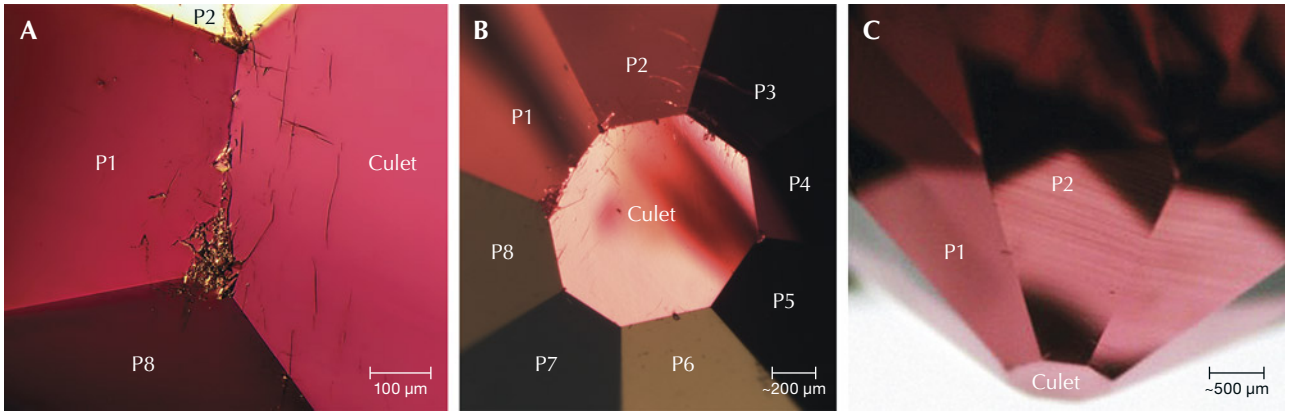

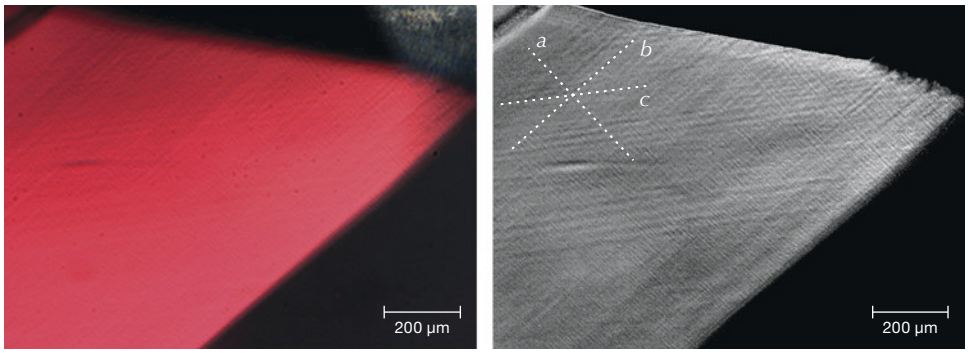

*Figure 8. Three directions of graining on a facet in true colors (left) and in black and white showing variations in hue (right). The three directions of graining (*a, b, *and* c*) are outlined in white dashed lines. Images by W. Henry Towbin.*

wise order (figure 7B). In this study, we focus on pavilion facet 2 (P2) for imaging and mapping techniques (figure 7C).

The face-up color of the stone appears homogeneous (again, see figure 1), but detailed optical microscopy revealed that the red color saturation is not homogeneous within the stone. This effect is most clearly observed when viewed through the pavilion facets, as seen in figure 7C. Three directions of red lamellae and thin bands, also known as graining, are visible. Colored graining and lamellae are associated with {111} oriented slip or glide bands. All three crystallographically equivalent directions of graining are visible in a plane-polarized view of a facet (figure 8, left), especially when the hues are represented in black and white (figure 8, right). Each direction of graining has a different periodicity, ranging from 9 to 13 µm along direction *a*, 15 to 23 µm along direction *b*, and 17 to 33 µm along direction *c* (figure 8, right). In at least one direction, the graining appears in bands with wavy textures, such as reported for Group 1 pink diamonds by Gaillou et al. (2012; see appendix 1 for more photos). Unlike Group 2 pink diamonds, in which the pink color is typically confined to the lamellae and surrounded by colorless layers in between, the Winston Red diamond is red throughout—but with deeper red saturation along the lamellae (figure 7C).

In at least one instance, two directions of the banding converge to create a hollow Rose channel that appears to be associated with an unidentified inclusion (figure 9, A and B). In pink diamonds, Rose channels are due to plastic deformation and are the consequence of the intersection of two directions of mechanical microtwinning (Schoor et al., 2016).

At first glance, the culet facet appears to have a chipped vertex (figure 7B), but microscopic observation reveals a box pattern similar to that of a coated diamond (Machado et al., 1985; Harris et al., 2022). We have interpreted this as the remnants of the rough diamond surface (figure 7A).

When viewed between cross-polarized filters, both mottled and wavy linear anomalous birefringence patterns could be observed, depending on the orientation (figure 9C). The dominant direction of linear anomalous birefringence features followed that of the lamellae and graining, but a pattern of finer linear features crossing through the primary direction could also be resolved. These observations have also been reported for Group 1 diamonds (Gaillou

Figure 9. A Rose channel with an inclusion in plane-polarized light (A) and cross-polarized light (B). Cross-polarized light showing two directions of graining and wavy patterns (C). Images by W. Henry Towbin.

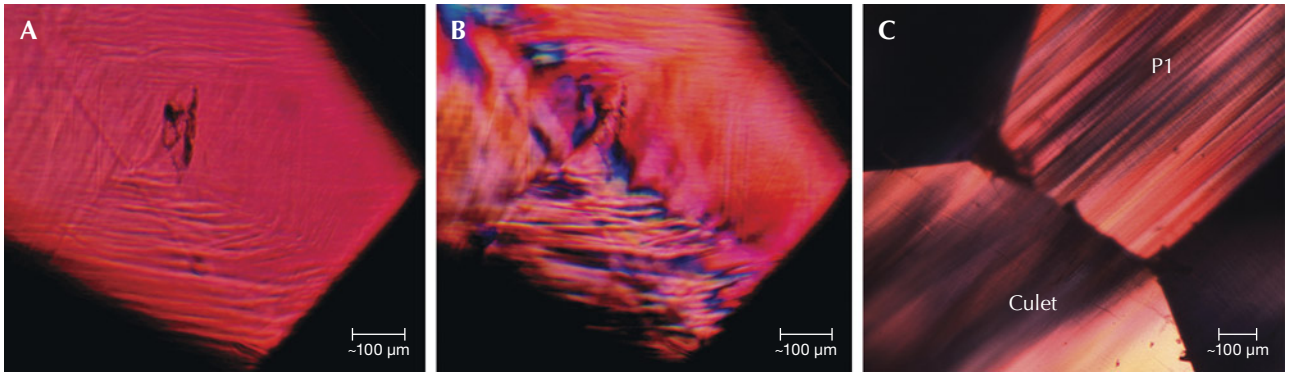

et al., 2012; Eaton-Magaña et al., 2020). High levels of strain were not restricted to discrete lamellae, unlike in Group 2 diamonds.

Characterization by FTIR and Vis-NIR Absorption Spectroscopy. *FTIR absorption spectroscopy.* FTIR spectroscopy was used to evaluate the presence of nitrogen-related defects in the Winston Red diamond. Aggregated nitrogen in both the A- and B-center forms were detected (nearest-neighbor nitrogen pairs and N_4V^0, respectively) in the resulting spectrum (figure 10, left), meaning that it can be classified as type IaAB (e.g., Breeding and Shigley, 2009). The most recognizable feature for A-centers is a broad peak at ~1282 cm^{-1}, whereas the B-centers are detected at ~1175 cm^{-1}. Concentrations were calculated with a Python script following the fitting methods of David Fisher's CAXBD97n Excel spreadsheet (De Beers Technologies, Maidenhead, UK), using the absorption coefficient relationships by Boyd et al. (1994, 1995) following spectral normalization based on the height of the two-phonon absorption in diamond (Palik, 1985). The total nitrogen concentration was determined to be 83 ± 8 ppm, with 76 ± 8 ppm B-centers and 7 ppm A-centers (i.e., 92% IaB). Additional absorption features include a sharp peak at 3107 cm^{-1} (N_3VH^0) (Goss et al., 2014) and broad bands around 4167 and 4839 cm^{-1} (most likely Amber Center 1; see Massi et al., 2005). Notably, the Amber Center 2 (4065 cm^{-1}) and the platelet peak, which can vary in position between 1358 and 1380 cm^{-1} (Woods, 1986; Speich et al., 2017), were not detected. Platelets are thin layers of carbon self-interstitial aggregates that form as A-centers convert to B-centers. Diamonds for which platelet concentrations are proportional to the B-center concentration are classified as "regular" according to Woods (1986). The absence of platelets for the Winston Red diamond would classify it as "irregular," which may suggest that they were broken apart by heating or significant deformation (Woods, 1986).

FTIR studies of pink diamonds by Gaillou et al. (2010) and Howell et al. (2015) suggest that Group 1 diamonds are type IaA<B with a relatively high aggregation state (%IaB>35%) and low total nitrogen concentrations that are generally below 200 ppm (but can extend up to ~800 ppm), as is similarly observed for the Winston Red diamond (figure 10, right, red diamond symbol). Meanwhile, Group 2 diamonds have a wider range of total nitrogen concentrations (150–1600 ppm) and relatively low aggregation (%IaB<35%). FTIR analysis of 399

Figure 10. Left: FTIR absorption spectrum of the Winston Red classifies it as a type IaAB diamond, with detectable concentrations of aggregated nitrogen as A-centers (nitrogen pairs, broad peak at ~1282 cm^{-1}) and B-centers (N_4V^0, ~1175 cm^{-1}). The weak broad bands around 3000 cm^{-1} are attributed to surface oil contamination. Right: Plot of the total nitrogen concentration vs. the nitrogen aggregation state (%IaB) for 399 Fancy red diamonds analyzed by FTIR at GIA, with the Winston Red diamond indicated with the red diamond symbol. Of this set, 156 of the diamonds originated from the Australian Argyle mine, whereas three were reportedly recovered in Minas Gerais, Brazil. The Winston Red diamond belongs to the Group 1 designation used for pink diamonds.

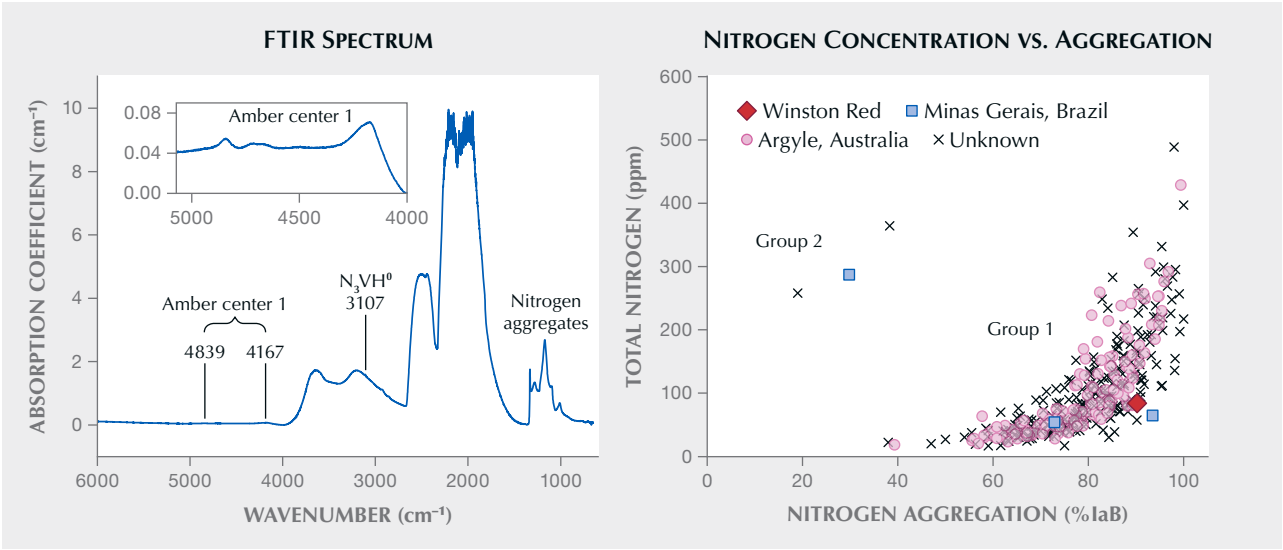

Fancy red diamonds submitted to GIA suggests that they overwhelmingly belong to Group 1, with only three samples (0.8%) showing total nitrogen concentration and aggregation states consistent with Group 2 diamonds (figure 10, right). For this sample set, 39.1% (156) of the diamonds are known to originate from Argyle, Australia, whereas 0.8% (3) were reportedly recovered in Minas Gerais, Brazil. The geographic origins of the remaining diamonds are unknown. These results may be biased by the high representation of type IaA<B pink to red diamonds from the prolific Argyle mine, and it is likely that the majority of the unknown samples share that origin (e.g., Rolandi et al., 2008; King et al., 2014; Eaton-Magaña et al., 2018). None of the red diamonds examined at GIA belong to Group 3 (type IIa, colored by 550 nm band), which encompasses 24% of natural pink diamonds (Eaton-Magaña et al., 2018, 2020). As with colorless diamonds, the larger pink diamonds are generally type IIa (S. Eaton-Magaña, pers. comm., 2024). It is possible that the saturated color associated with Fancy red diamonds cannot be achieved in type IIa diamonds. If so, this incompatibility may also explain the relatively modest sizes attained by red diamonds.

Vis-NIR Absorption Spectroscopy. Vis-NIR absorption spectroscopy collected at liquid nitrogen temperature was used to investigate the color centers responsible for the Winston Red diamond's Fancy red grade (figure 11; see also table 3). The dominant feature observed is a broad asymmetric absorption band centered at around 550 nm, along with nitrogen-related absorption from N3 (N_3V^0, zero phonon line, or ZPL, at 415 nm), H4 ($N_4V_2^0$, ZPL at 496 nm), and H3 (N_2V^0, ZPL at 503.2 nm) centers (e.g., Green et al., 2022). This gives rise to a transmission window in the red part of the visible spectrum, producing the diamond's characteristic color. The 550 nm absorption band is responsible for the pink color in over 99% of natural pink-hued diamonds, as well as all natural red diamonds that have been graded at GIA (Eaton-Magaña et al., 2018, 2020; also confirmed by the current authors). The absorption intensity of the 550 nm band, as well as the diamond's size and cut, determine the color saturation and whether it will be predominantly pink or red (King et al., 2002; Eaton-Magaña et al., 2018). The subtle balance of the 550 nm band and the N3, H4, and H3 absorption features are responsible for the Winston Red's pure unmodified red color. Although this 550 nm band has been associated with

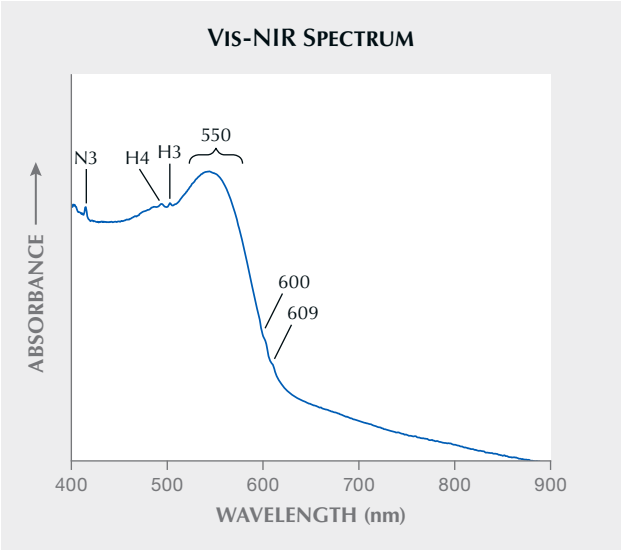

Figure 11. The Vis-NIR absorption spectrum of the Winston Red diamond is dominated by a strong 550 nm band, along with absorption by N3 (415 nm), H4 (496 nm), and H3 (503.2 nm) centers. Weak absorption from the "609 nm system" is also detected. Data was collected at 77 K with the sample in its equilibrium color state, prior to any significant ultraviolet light exposure that could induce photochromism.

plastic deformation, the defect structure has not yet been determined (e.g., Orlov, 1977; Collins, 1982; Gaillou et al., 2010; Howell et al., 2015; Eaton-Magaña et al., 2018, 2020). The band is observed in both pink type Ia (Groups 1 and 2) and type IIa (Group 3) diamonds, suggesting that nitrogen content is not directly linked to the pink color centers. However, this does not rule out that the presence of nitrogen may still be indirectly involved in pink color formation. In pink diamonds, the 550 nm band is typically observed along with a band at 390 nm (e.g., Eaton-Magaña et al., 2018); however, its presence could not be confirmed for the Winston Red diamond because the collected spectrum did not extend below 400 nm. Peaks at 609 and 600 nm, associated with the "609 nm system" first defined by Fritsch et al. (2007), are weakly observed, overlapping with the low energy tail of the broad 550 nm band. The 609 nm system, which presents as a series of oscillations spanning between ~550 and 609 nm, has been reported for pink diamonds colored by the 550 nm band, being most noticeable in low-nitrogen or type IIa pink diamonds (Shigley and Fritsch, 1993; Fritsch et al., 2007; Eaton-Magaña et al., 2018, 2020). This 609 nm emission system possibly mirrors the 550 nm absorption band and might be due to the same unknown defect (Eaton-Magaña et al., 2020). Due to

TABLE 3. Absorption and PL spectroscopy features in the Vis-NIR range for the Winston Red diamond.

Feature (nm)	Feature (eV)	Spectroscopic technique	Description
415.2	2.986	Absorption, PL	N_3V^0, known as N3
490.7	2.527	PL	Observed in plastically deformed diamond
494.5	2.507	PL	Unknown
496.2	2.499	Absorption, PL	$N_4V_2^0$, known as H4
503.2	2.464	Absorption, PL	N_2V^0, known as H3
535.8	2.314	PL	Possibly interstitial-related; commonly observed in diamonds with B-centers
550	2.254	Absorption	Broad band associated with pink color in natural diamonds; thought to arise from plastic deformation
552.7	2.243	PL	Unknown
576	2.152	PL	Unidentified defect that is not the NV^0 (575 nm) center
586.9	2.112	PL	Unknown
600.7	2.064	PL	Unknown
609 (600, 594, 586, 573)	2.036	Absorption	"609 system" seen in pink diamonds, with oscillations to lower wavelength; possibly linked to the 700 nm emission band (see Fritsch et al., 2007 and Eaton-Magaña et al., 2020)
616.5	2.011	PL	Unknown
626.1	1.980	PL	Unknown
646.8	1.917	PL	Unknown
654.9	1.893	PL	Unknown
660.8	1.876	PL	Commonly seen in pink diamonds
668.7	1.854	PL	Commonly seen in pink diamonds; possibly Ni-related
700	1.771	PL	"700 nm emission band," also referred to as the 600–750 nm emission band; includes oscillations to lower wavelength and possibly linked to the 609 nm system seen in absorption (Eaton-Magaña et al., 2020)
710	1.746	PL	Observed in some pink diamonds
731.4	1.769	PL	Possibly related to interstitial nitrogen
741	1.673	PL	V^0, known as GR1
890	1.393	PL	Unknown
900	1.378	PL	Unknown
915	1.355	PL	Unknown

their extreme rarity, few Fancy red diamond UV-Vis-NIR absorption spectra have been published (Shigley and Fritsch, 1993; Eaton-Magaña et al., 2018); these reports also show intense absorption in the 550 nm band, coupled with comparatively weak absorption from N3, H4, and H3 centers, consistent with the Winston Red diamond.

Luminescence Spectra and Imaging. *Photoluminescence Spectra.* Non-confocal photoluminescence measurements using various laser wavelengths (405, 457, 514, 633, and 830 nm) captured an array of luminescent features in the Winston Red diamond, as shown in figure 12 and detailed in table 3. The 405 nm–excited PL spectrum was collected at room temperature and the remaining data with the sample liquid nitrogen–cooled to 77 K. The spectrum collected with the 405 nm laser is dominated by the N3 defect, with weak H3, as would be expected based on their detection in the stone's Vis-NIR absorption spectrum (figure 12), combined with the weak concentration of luminescence-quenching A-centers detected by FTIR absorption (again, see figure 10) (Thomaz and Davies, 1978). Several of the PL features detected for the Winston Red are commonly observed in the luminescence spectra for pink diamonds colored by the 550 nm absorption band (e.g., Iakoubovskii and Adriaenssens, 2002; Gaillou et al., 2010; Eaton-Magaña et al., 2018, 2020). Notably, the 514 nm laser effectively excited an intense broad luminescence band that peaks at around 700 nm, dominating the 500–850 nm wavelength range (figure 12C). Eaton-Magaña et al. (2018, 2020) demonstrated that the intensity of this emission band correlates with the 550 nm absorption band, suggesting that it can be used as a proxy for this absorption. The "pink emission band" includes a series of characteristic oscillations that also possibly relate to the 609 nm system in absorption, seen in figure 11 (Eaton-Magaña et al., 2018, 2020). The 700 nm emission band, also referred to as the 600–750 nm emission band, has been shown to have consistent peak positions (Eaton-Magaña et al., 2020). The 490.7 nm, H4, H3, 576 nm, and 668.7 nm luminescence peaks observed for the Winston Red have previously been associated with Group I (type IaA<B) pink diamonds, being less common for those belonging to Group 2 (type IaA>B) (Eaton-Magaña et al., 2020). The 490.7 nm defect is thought to be nitrogen-related and a product of plastic deformation (Collins and Woods, 1982). Other notable features are the 535.8, 654.9, 660.8, and 710 nm peaks. The former is commonly seen in diamonds with B-centers and may be interstitial-related (Laidlaw et al., 2021), consistent with the Winston Red's diamond type. A weak strain-broadened GR1 (neutral vacancy, V^0, ZPL at 741 nm) is also detected (Iakoubovskii and Adriaenssens, 2002; Gaillou et al., 2010). The 830 nm laser excited unidentified broad bands centered at 890, 900, and 914 nm.

The authors are not aware of any published PL spectra for natural Fancy red diamonds, so this study presented an opportunity to explore data collected internally at GIA for 10 client-submitted diamonds using similar excitation wavelengths. Comparison of the spectra for the Winston Red and the Fancy red diamond suite reveals the clearest similarities when excited by the 633 nm laser. The 654.9, 660.8, and 668.2 nm peaks were always detected together, though their intensities do not correlate, suggesting that they do not share a common defect origin. The 660.8 nm peak appears to be a zero-phonon line with vibronic structure that results in a series of broad bands at higher wavelengths, with the most distinctive peaking at ~682, 691, and 703 nm, as determined by comparing the peak ratios for all samples they were detected in. The vibronic structure associated with the 660.8 nm peak fell below the detection limit of the spectrum collected for the Winston Red diamond and cannot be seen in figure 8, left. The 710 nm peak, which dominates the 633 nm excited PL for the Winston Red (figure 12D), was detected for 80% of the other Fancy red diamonds. Notably, the spectra for all the other Fancy red diamonds show a peak at 731.4 nm that was not observed for the Winston Red. The 731.4 nm peak has been attributed to a characteristic of interstitial nitrogen (Deljanin et al., 2008). GR1 was detected for all these samples. Spectra collected with the 514 nm laser show more variability, with only the spectrum for the Winston Red diamond displaying a clear 700 nm band—the others appear to include an additional overlapping band that rises steeply from ~500 nm and peaks at ~600 nm. However, we do note that all the samples showed an emission at 535.8 nm, with nearly all also showing emissions from H3, H4, and 576 nm peaks (typically one peak being absent). Finally, PL spectra collected with the 830 nm laser revealed that all the diamonds for which the 710 nm emission was detected also showed unidentified broad peaks at 890, 900, and 914 nm, with varying intensities. Although this sample set is limited, it was sufficient to demonstrate a range of peaks commonly observed for Fancy red diamonds, yet it did not unravel any distinctive trends between the peaks.

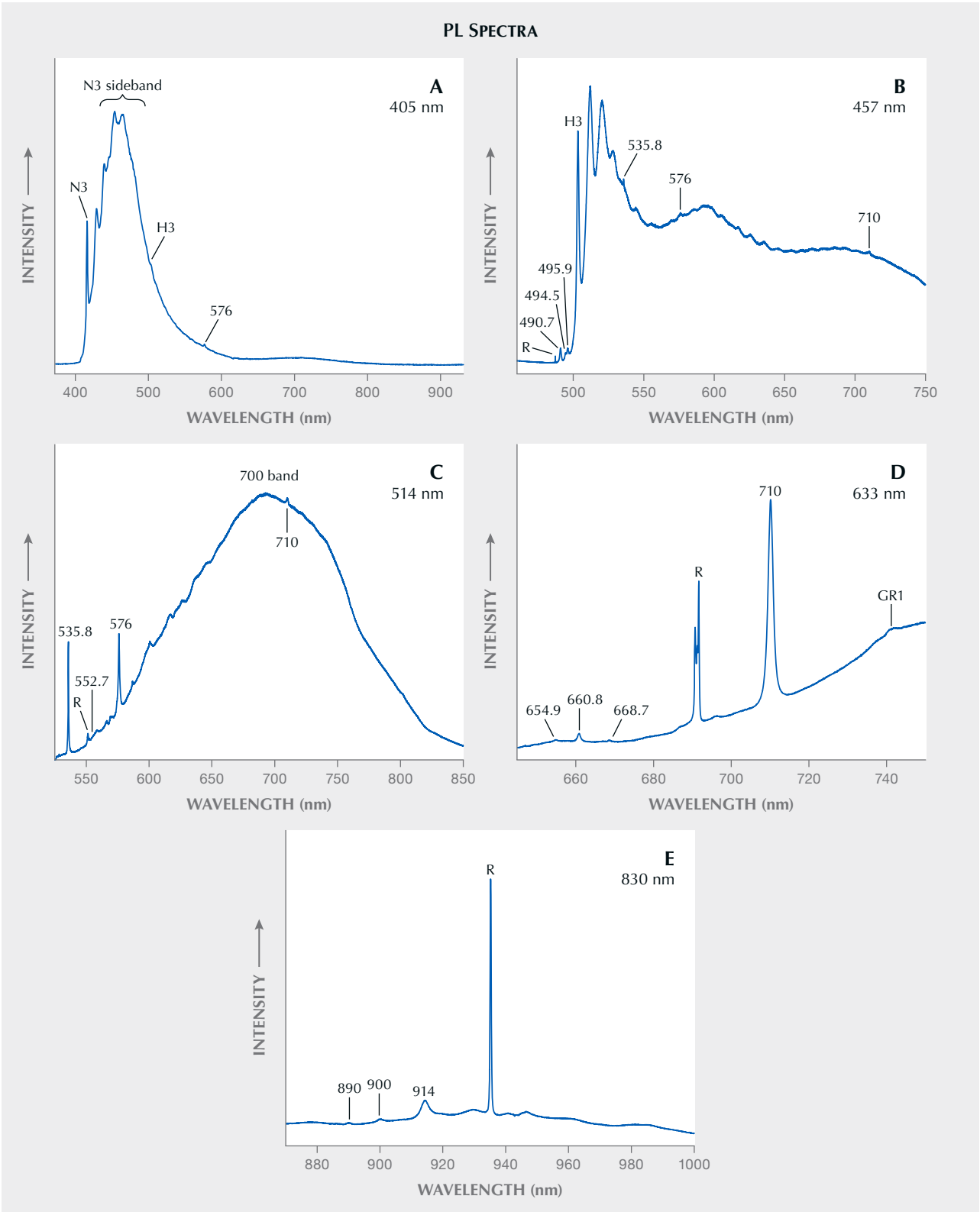

Figure 12. Photoluminescence spectra of the Winston Red diamond using 405 nm (A), 457 nm (B), 514 nm (C), 633 nm (D), and 830 nm (E) lasers. All spectra except for A were collected with the sample cooled to 77 K. Spectra B–D were Raman normalized to the integrated intensities of the diamond Raman peaks (R); the splitting of the Raman peak in D is a result of the excitation laser line shape.

Fluorescence Observations and DiamondView Imaging. The Winston Red diamond's fluorescence was first investigated during its grading at GIA in 2023 using long-wave UV (365 nm) illumination, an identifying characteristic described in its grading report as "faint" blue (again, see figure 2). This blue fluorescence arises from the N3 defect (also excited by the 405 nm laser in figure 12A) and has been detected in ~93% of the Fancy red diamonds graded at GIA.

Weak heterogeneous green fluorescence was observed for the Winston Red when illuminated with a color-neutral halogen light from a fiber-optic probe (SCHOTT KL 1500 HAL Fiber Optic Light Source Illuminator) during microscopic examination, with the emission following the stone's graining. This effect, commonly known as "green transmission," is caused by the emission of H3 centers and was also reported for the DeYoung Red (Shigley and Fritsch, 1993). The fiber-optic light source emits weakly below 415 nm and is more efficient at exciting fluorescence from H3 centers than from N3 centers (Luo and Breeding, 2013). Green transmission has been noted for ~60% of the Fancy red diamonds inspected at GIA.

When viewed under deep-UV (<225 nm) illumination from the DiamondView device, the Winston

Figure 13. DiamondView images of the Winston Red's table (A and B) and selected pavilion facets (C and D). The reference images on the left (A and C) and the fluorescence images on the right (B and D) were collected under white light and deep-UV illumination, respectively. The distribution of the blue N3 fluorescence reveals the diamond's intrinsic growth pattern. The inset of an area outlined in black lines in D shows the graining features as best observed using the red filter (725 nm long-pass). Comparison of the diamond's color for images A and C highlights its reversible photochromism, changing to a brown color following UV exposure. The white rectangle in D indicates a region that was further explored using photoluminescence mapping techniques. Images by Ulrika F.S. D'Haenens-Johansson.

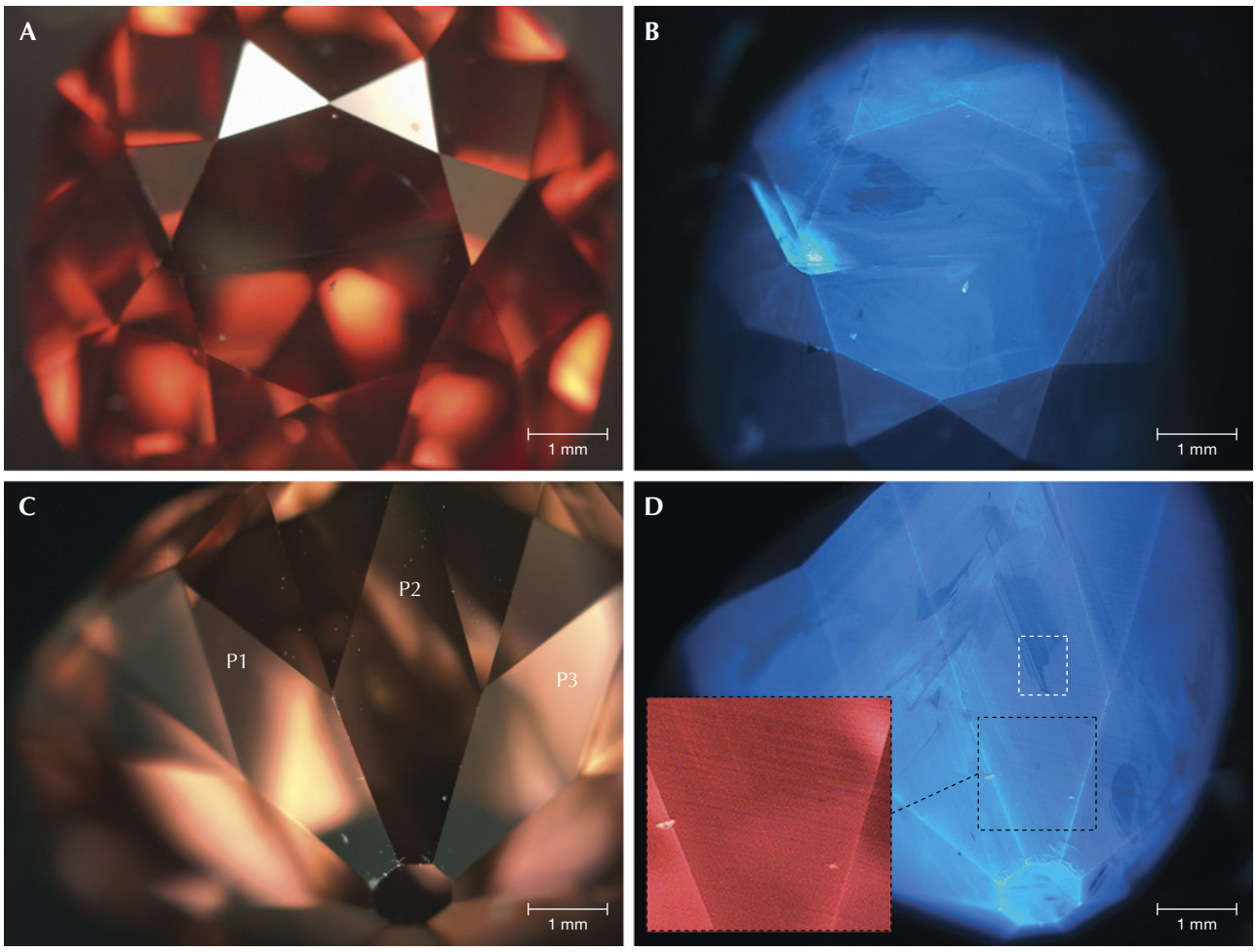

Red diamond displays blue fluorescence from N3 centers (figure 13), revealing a natural growth pattern. Along the pavilion facets, linear features that follow the lamellae (figures 7C and 13D) can be weakly resolved crossing through various growth zones—evidence of plastic deformation. The dominance of the N3 fluorescence under this excitation wavelength means that the colored filter detection accessories mainly transmit in its high wavelength "tail" (refer to the 405 nm–excited PL spectrum in figure 12A) and hence do not provide clear information on the identity and distribution of other fluorescing defects.

The Winston Red diamond—similar to pink and red diamonds colored by the 550 nm band—is photochromic. Illumination with ultraviolet light (long-wave, short-wave, or deep-UV from the DiamondView) results in a temporary color change, reducing the depth of color and imparting an orangy brown hue to the red stone. This can be clearly seen when comparing the color of the diamond in the white light images before and after deep-UV exposure (figure 13, A and C, respectively). Studies of the photochromism of the 550 nm absorption band sometimes refer to the color change following UV exposure as "bleaching," yet the effect varies, resulting in color changes toward yellow, brown, or orange hues, or a simple reduction in color saturation (e.g., Fisher et al., 2009; Byrne et al., 2012, 2014; Eaton-Magaña et al., 2018, 2020). The brown hue observed in the Winston Red diamond following UV exposure may be related to an underlying absorption continuum that relates to the Amber 1 centers detected by FTIR absorption (again, see figure 10). The color change is reversible, with exposure to longer wavelengths (>530 nm) or strong white light leading to color recovery. If kept in the dark, the "bleached" state may be maintained for an extended period of time. Though this was not tested for the Winston Red, Byrne et al. (2012) estimated that the color recovery of bleached pink diamonds that are kept in the dark at room temperature may take on the order of 100 days.

Hyperspectral Photoluminescence Imaging. The distribution of luminescing centers on the pavilion facet noted as P2 in figures 7 and 13 were investigated in more detail by photoluminescence mapping of N3, the 576 nm peak, and the 700 nm broad band (integrating over the spectral window 625–677 nm) emissions (figure 14). This facet was selected as it showed visible color graining, as well as growth and plastic deformation–related structures in the fluorescence images. N3 was excited using a 405 nm laser, whereas the remaining two centers were excited by a 532 nm laser. With the available excitation wavelengths, it was not possible to excite H4 or H3 without simultaneously exciting the significantly stronger N3; hence the distribution of these centers was not considered. N3, the 576 nm peak, and the 700 nm emission band show wavy linear distributions following two primary directions. The intensity variations are subtle for N3 and more pronounced for the 576 nm peak and 700 nm emission band. The N3 defect will strongly correlate to the initial growth of the diamond, incorporating different concentrations of nitrogen, which eventually form N3, creating

Figure 14. PL mapping of various spectroscopic features on the P2 facet defined in figure 7. On a small region near the facet junction on the right side of P2: peak area of the N3 ZPL at 415 nm normalized to the Raman peak area (A), peak area of the 576 nm ZPL (B), and emission area of the 625–677 nm region associated with the broad band centered at ~700 nm (C).

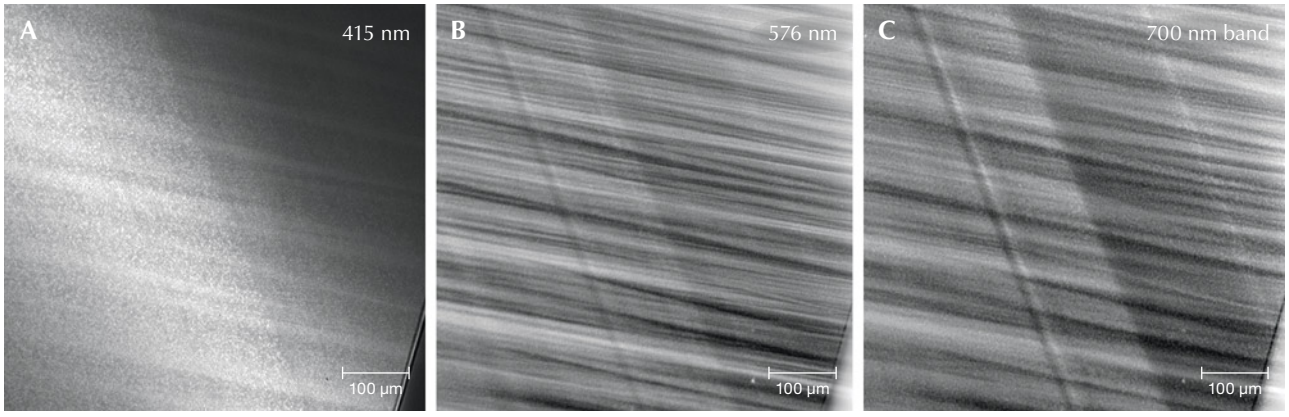

growth bands, while the 576 and 700 nm features are more directly related to plastic deformation. Although there are similarities between the luminescing defect distributions, they do not match exactly. Notably, they were not solely restricted to sharp, straight lamellae or slip planes. The approximately linear patterns cross uninterrupted through different growth zones, as seen in figure 15, indicating that they are the result of post-growth processes such as natural plastic deformation. A granular or "fish-scale" pattern can also be resolved (Gaillou et al., 2012), with the grains being bright with dark outlines, which is more pronounced in the PL maps for N3 and the 700 nm band.

Eaton-Magaña et al. (2020) explored the distribution of the 490.7 nm, H4, H3, and 576 nm peaks, as well as the 700 nm band, in pink Group 1 (type IaA<B) and Group 2 (type IaA>B) diamonds. For Group 1 pink diamonds, they found that luminescence intensities increased within the wavy pink lamellae, tracking with higher color concentrations, yet they noted detectable intensities between lamellae. This was considered consistent with pink coloration observed throughout the stone. The Group 2 pink diamonds did not show as many luminescent defects, and the discussion was restricted to the distribution of H3 and the 700 nm band. Emissions from these centers were segregated to the color-restricted straight lamellae. The distributions of luminescing features for the Winston Red diamond are similar to those reported for Group 1 pink diamonds.

Cathodoluminescence and Secondary Electron Imaging. Cathodoluminescence imaging of the Winston Red diamond corroborates many of the features that we observe with optical, fluorescence, and hyperspectral PL imaging (figure 16). The blue CL

Figure 15. Following similar analytical procedures, a region encompassing a distinctive growth zone as outlined in white in figure 13D is PL mapped for N3 (A), the 576 nm peak (B), and the 700 nm band (C). The yellow arrow in A shows an area at the edge of the growth zone that is devoid of N3. D–F: The same information shown in A–C is repeated for the region outlined in white in image A.

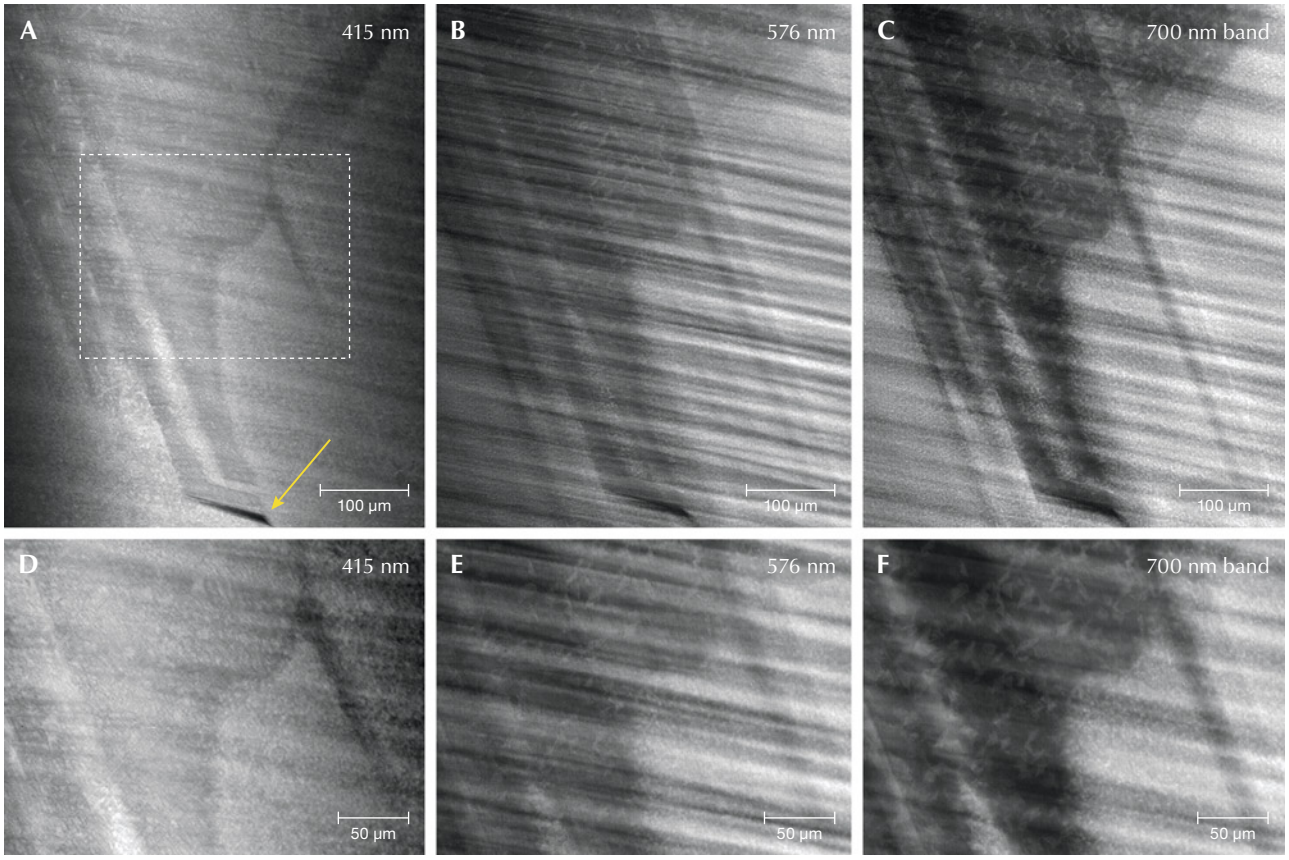

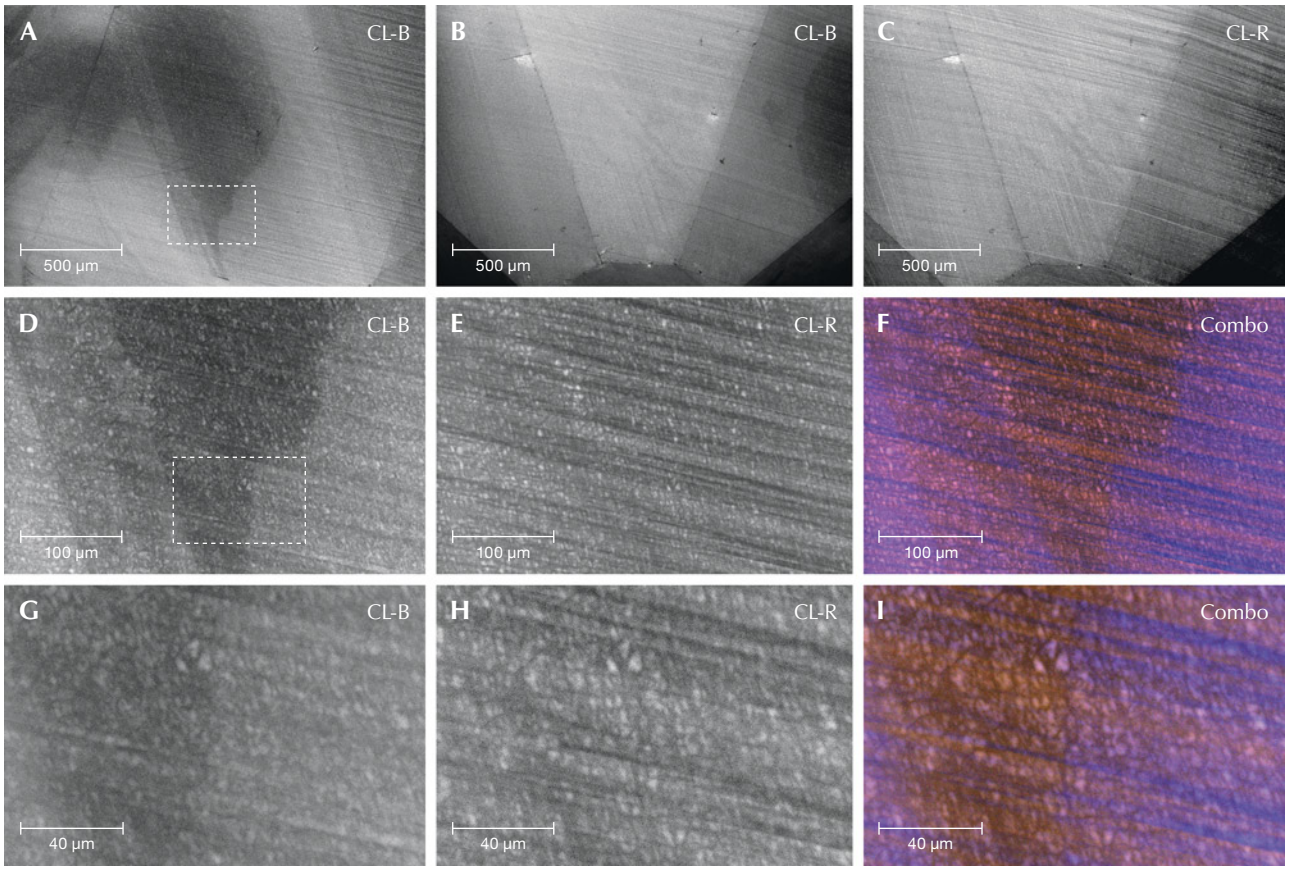

Figure 16. SEM-based cathodoluminescence imaging. A: Pavilion facet 2 (P2) is imaged with the blue CL channel in the center of P2 to show a growth feature, similar to what is seen in the DiamondView (figure 13D). The region near the culet of P2 is imaged with the blue CL channel (B) and the red CL channel (C; to better show the lamellae). At higher magnification in the region outlined in A, the blue CL channel (D) shows the growth pattern and begins to reveal fish-scale dislocation network patterns (granular textures), while E clearly shows the lamellae. F: A combined image of the red, green (not shown), and blue CL channels shows the growth feature, the lamellae, and the dislocation networks. G–I: Follow the same order of features as D–F, but at higher magnification for the region outlined in white lines in D.

channel, similar to the DiamondView blue filter, clearly reveals growth zones (figure 16, A and B), especially at higher magnifications (figure 16, D and G). Although it was not possible to confirm by CL spectroscopy, the intensity variations captured by this channel are primarily associated with the N3 defect, showing patterns consistent with the DiamondView fluorescence (figure 13, B and D) and hyperspectral PL images (e.g., figure 15A). Blue "Band A" emission (broad band ~400–500 nm) associated with unidentified defects located in the material adjacent to dislocations may also contribute to the signal (Dean, 1965; Ruan et al., 1992; Gaillou et al., 2012; Laidlaw et al., 2021). Slip bands associated with the graining are weakly detected. Images collected with the green channel did not reveal any significant differences, likely capturing the high-wavelength tail of the N3 emission (not shown) rather than weaker emissions by H4, H3, or 576 nm defects, consistent with green filtered DiamondView imaging observations.

The various directions of graining observed with optical and DiamondView imaging show up very clearly with the red CL channel (figure 16C). The red CL channel images fail to reveal the growth features shown by the blue CL channels (figure 16, E and H), possibly suggesting that the luminescence it captures is not directly related to the nitrogen uptake of the growth zone. Instead, they show a similar periodicity in lamellae as observed in the optical grayscale hue

image (figure 8, right). The combination of the blue and red channel signals showcases the complex growth and deformation-related features, such as the slip bands and dislocation networks, in the Winston Red diamond (figure 16, F and I).

An interesting discovery for the Winston Red diamond is the presence of cellular dislocation networks and subgrain boundaries that can be resolved by PL mapping and CL imaging (figure 14A; figure 15, A and D; and figure 16, D–I). The dislocations effectively quench the luminescence from the color centers (Laidlaw et al., 2021), resulting in a granular texture that extends across different growth zones and slip bands. At the magnifications employed in this study, the density of the granular texture did not noticeably change between the slip bands. Transmission electron microscopy imaging of cellular dislocation networks in plastically deformed brown type IIa diamonds shows that the boundaries between the grains or cells are composed of high concentrations of dislocations (Laidlaw et al., 2021). Laidlaw et al. also reported clear differences in the dislocation microstructure between brown and colorless regions of the same sample. Previous pink diamond studies have also observed the cellular dislocation networks in low-nitrogen type IaA<B diamonds, enveloping grains with yellowish green luminescence from H3 centers (Gaillou et al., 2010, 2012). These patterns are most commonly observed in Group 1 pink diamonds, such as those from Argyle (Australia), Santa Elena (Venezuela), and marine deposits in Namibia (Gaillou et al., 2010, 2012; Howell et al., 2015). Referred to as "fish-scale" patterns, they were attributed to interactions between two or more directions of strain. The Winston Red diamond has similarly experienced deformation along several directions, as evidenced by its cross-cutting lamellae and Rose channels in figures 8, 9, 14, and 15.

Surprisingly, these cellular dislocation networks seem to have influenced the topography of the Winston Red diamond's facets, as seen with SEI (figure 17). Faint linear features consistent with slip planes can also be resolved. This topography may have been produced by differences in the hardness of the regions with high concentrations of dislocations. Note that the surface features presented in figure 17 (right) are observed at higher magnification than the CL images shown in figure 16.

Origin of the Color in the Winston Red Diamond. The Winston Red diamond exhibits a saturated red color that is homogeneous to the unaided eye (again, see figure 2). However, it is heterogeneous under magnification, following the graining in thin alternating red bands along three different directions (again, see figure 8). In some areas, a wavy red pattern is also observed. Although the distribution is not uniform, the regions between these lamellae also show pink or red color. The observed color is primarily due to an intense broad absorption band at 550 nm, with contributions from nitrogen-related N3 (N_3V^0), H3 (N_2V^0), and H4 ($N_4V_2^0$) defects (e.g., Orlov, 1977; Collins, 1982; Gaillou et al., 2010; Howell et al., 2015; Eaton-Magaña et al., 2018). The wavy appearance of the color graining in the Winston Red diamond, coupled with its type IaA<B classification and

Figure 17. Left: Secondary electron imaging (SEI) showing how dislocation network patterns are expressed at the surface of the diamond in the same region as in figure 16G. The box shapes are from the electron beam having rested at those regions at higher magnifications. Right: Higher magnification imaging reveals further details for the dislocation network patterns and lamellae.

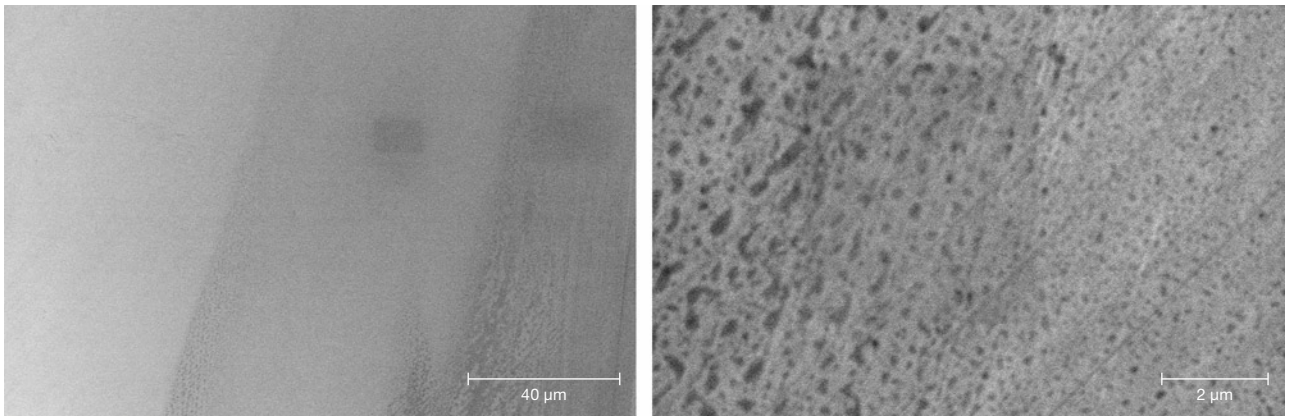

characteristic distribution of luminescing centers, show that it belongs to the pink diamond Group 1 designation, with the Fancy red color being a result of a high concentration of "pink" defects, coupled with the sample's size and cut.

The production of pink and brown colors in diamonds is closely associated with plastic deformation, and both hues frequently coexist (e.g., Eaton-Magaña et al., 2018). The timing and geological conditions that cause the shear stresses and temperatures necessary for plastic deformation resulting in pink and/or brown colors are still under debate (Smith, 2023). Diamond's explosive magmatic ascent may result in plastic deformation and the production of these defects (e.g., Fisher, 2009). Yet it is also possible that the deformation associated with these colors occurred earlier during mantle residency, where diamonds may have experienced temperatures between 900° and 1400°C (Stachel and Harris, 2008; Nimis, 2022). DeVries (1975) demonstrated that plastic deformation and microtwinning can occur at temperatures above 900°C, though deformation at temperatures as low as 770°C has also been reported (Brookes et al., 1999). After color is formed in the diamond, color preservation depends on the original defect concentrations, temperature, and time (Fisher, 2009; Fisher et al., 2009; Smith et al., 2010). Following or concurrent with deformation, exposure to high temperatures over many millions of years may also result in defects annealing out (Fisher, 2009; Fisher et al., 2009). Annealing experiments on natural brown type IIa diamonds have shown that the 550 nm band defect has a higher thermal stability than the vacancy clusters associated with the brown color, and that pink color can intensify as brown color anneals out (Fisher, 2009; Fisher et al., 2009). In summary, the Winston Red diamond likely required a perfect geological journey in order to produce and preserve such an intense red color.

Here we explore possible causes of pink and red color production and consider why Group 1 pink to red diamonds, like the Winston Red, often have colors that are more saturated and homogeneous than those reported for Group 2 diamonds (Gaillou et al., 2012; Eaton-Magaña et al., 2020). Notably, analysis of hundreds of Fancy red diamonds submitted to GIA emphasizes the prevalence of Group 1 diamonds and the extreme rarity of Group 2 diamonds (0.8%; 3 of 399 Fancy red diamonds) (figure 10, right). While the structure of the color center of the 550 nm absorption band primarily responsible for pink and red colors in diamond is still unknown, it is associated with plastic deformation. Plastic deformation can generate and move dislocations in diamond and/or create mechanical twins. However, neither dislocations nor microtwins themselves are responsible for (significant) color as they can also be observed in high concentrations in colorless diamond. Due to the frequent coexistence of brown and pink colors, the latter defect may have a similar structure to the vacancy clusters responsible for brown color (Fisher, 2009; Fujita et al., 2009; Jones, 2009; Mäki et al., 2009; Guagliardo et al., 2013). It is also possible that the movement of dislocations through plastic deformation may modify preexisting defects, creating new structures that produce pink color (Fisher et al., 2009; Laidlaw et al., 2021). The detection of the 550 nm absorption band for "nitrogen-free" type IIa diamonds (Group 3) suggests that the defect responsible may not necessarily include nitrogen, yet it is possible that the mechanism for its production is still affected by nitrogen.

Nitrogen content, preexisting dislocations, and other defects such as platelets are known to influence plastic deformation in diamonds (Evans and Wild, 1965, 1966; Wild et al., 1967; Brookes et al., 1999, 2000; Brookes and Daniel, 2001; Fisher et al., 2009). Nitrogen and platelets are thought to restrict the movement of dislocations during plastic deformation, which in natural type I diamonds are generally concentrated along {111} slip and glide planes (Evans and Wild, 1965, 1966; Wild et al., 1967). Both Group 1 and Group 2 pink diamonds are type Ia, yet those belonging to Group 1 are characterized by lower total nitrogen concentrations that are heavily aggregated, along with reduced platelet concentrations that would typically classify them as "irregular" (Woods, 1986; Gaillou et al., 2012; Howell et al., 2015). Their lower concentrations of total nitrogen and platelets may make them more ductile than Group 2 pink diamonds, facilitating plastic deformation.

It is also possible that Group 1 diamonds may have experienced more extreme deformation and natural annealing events than Group 2 diamonds (e.g., multiple events, higher temperatures, and/or prolonged time frames), resulting in their polygonized dislocation networks, higher nitrogen aggregation states, and relatively low (or absent) platelet concentrations (Sumida and Lang, 1981; Woods, 1986; Howell et al., 2015; Nimis, 2022). If the formation mechanism for the 550 nm absorption band defect involves the movement of dislocations, the

presence of polygonized dislocations between slip bands in Group 1 diamonds may be tied to the pink to red colors observed between lamellae (figure 7C) and the overall more even color compared to Group 2 diamonds.

In the case of Group 2 pink diamonds—which do not show polygonized dislocations—the pink color is concentrated around mechanical microtwins (pink lamellae) (Mineeva et al., 2007, 2009; Gaillou et al., 2010; Howell et al., 2015). Howell et al. (2015) suggested that microtwinning events are key to pink color production and speculated that the absence of direct evidence for microtwinning in Group 1 pink diamonds could be explained by "detwinning processes," possibly occurring during secondary deformation events. These hypotheses require future testing with diamonds of different nitrogen contents and aggregation states, under strain and temperature conditions similar to those in Earth's mantle. Additionally, studying more diamonds of known geographic origins would provide more concrete clues to tie pink diamond groups and colors to craton age and geological history.

In summary, the origin of the red color in the Winston Red diamond appears to be linked to two factors: relatively low nitrogen concentrations that facilitate plastic deformation, and exposure to high pressure and temperature conditions that led to significant dislocation generation and movement along several directions, resulting in the production of high concentrations of pink color–producing defects throughout the diamond. Additionally, the temperatures that the diamond experienced must have been insufficient to anneal and destroy the 550 nm band defect that produced the pink color (Fisher et al., 2009). This combination of features illustrates the unique crystallization, geological residence, and transportation history necessary for the Winston Red diamond's beautiful saturated red color.

The Geographic and Geologic Origin of the Winston Red Diamond. Historical records do not provide a geographic source for the Winston Red diamond, but the new data presented here offer some clues that unveil a likely origin. Unlike for some gem minerals, the geographic origin of gem-quality diamonds that formed deeper in Earth's relatively geochemically homogenous mantle cannot be determined based on the usual combination of inclusions, spectroscopic characteristics, and chemistry (e.g., Smith et al., 2022). Other gems are predominantly formed in the continental crust and bear characteristic signatures (e.g., inclusions) of their host rocks and geological environment. In diamonds, inclusions may give clues to paragenesis (e.g., peridotitic or eclogitic), age, and formation depth (>140 km). The Winston Red diamond contains only a few visible inclusions that are too deep inside it to identify with Raman spectroscopy (figures 2 and 9).

For pink and red diamonds, the story is slightly different. It has been demonstrated that two geological settings produce pink and red diamonds: Group 1 formed in Proterozoic (0.5–2.5 Ga) cratons, while Group 2 formed in Archean (2.5–4 Ga) cratons (Gaillou et al., 2012; Howell et al., 2015). No known primary deposits contain both Group 1 and Group 2 diamonds; however, the study of pink diamonds of known localities is limited. Information on Group 3 (type IIa colored by the 550 nm band) pink diamonds is even more rare (Eaton-Magaña et al., 2020). The current article presents FTIR data for nearly 400 Fancy red diamonds analyzed at GIA (figure 10, right), including 39.1% originating from Argyle, Australia, and 0.8% reportedly from the Minas Gerais region of Brazil.

As discussed above, the visual and spectral characteristics of the Winston Red are consistent with Group 1 diamonds. Group 1 pink diamonds with these characteristics have been reported from Argyle in Australia, Santa Elena in Venezuela, and the marine deposits in Namibia (e.g., Gaillou et al., 2010, 2012; Howell et al., 2015). Kaminsky et al. (2000) were the first to link diamonds from Venezuela (placers from the 730 Ma Guaniamo kimberlites) and Argyle (primary deposit in the 1180 Ma Argyle lamproite), as they had similar mineralogical features and geological environments. Diamonds from these deposits have a high proportion of inclusions associated with an eclogitic paragenesis and are mostly type IaA<B with low nitrogen concentrations. They formed at the bases of Proterozoic cratons that may contain a significant proportion of eclogites, formed by subduction of the continental crust. Both underwent strong tectonothermal events, with intrusions of magma and/or rifting, which are different from the more ancient Archean cratons.

As mentioned earlier, we can now trace the history of the Winston Red diamond to 1938 and suspect that, based on the old mine cut, the stone was discovered even earlier. Since we have determined that the Winston Red is a Group 1 stone, sources of Group 2 pink and possible red diamonds can be excluded, such as South Africa, Russia, Tanzania, and Canada (Gaillou et al., 2012), with the

latter two additionally having been discovered too recently. As far as we are aware, no red diamonds have been reported from India, an important historic source of diamonds. Indian pink diamonds tend to be faint to light pink type IIa colored by NV centers or the 550 nm band (Group 3) (Eaton-Magaña et al., 2018, 2020). Thus, this locality may be excluded as well. Considering Group 1 diamonds, the most commonly prolific source of pink and red diamonds is the Argyle mine. FTIR analysis of 156 Fancy red diamonds from Argyle submitted to GIA indicates that they, too, belong to Group 1. However, Argyle diamonds were first discovered in 1979 (e.g., Shigley et al., 2001); thus, this origin can be ruled out for the Winston Red. Diamonds in marine sediments from Namibia were first reported as early as the end of the nineteenth century (Schneider, 2020). A few diamonds were recovered in 1910 on Possession Island, but the operation was shut down the same year due to economic pressures. Further prospecting of the Namibian seashore began in 1958, with production beginning in the 1960s (Schneider, 2020). As for Venezuelan diamonds, several alluvial sources in the state of Roraima have been reported as early as 1890 (Harlow, 1998). Thus, Venezuela is a potential source.

Brazil is another well-known historic locality for producing pink and red diamonds, including the famous 5.11 ct Moussaieff Red diamond cut from a 13.90 ct crystal recovered from an alluvial deposit in Noroeste de Minas, Minas Gerais, Brazil, in the mid-1990s (e.g., King et al., 2002; King and Shigley, 2003; Svisero et al., 2017; Hoover et al., 2018). Unfortunately, limited information is available for this diamond, though it is noted as type Ia (no nitrogen content or aggregation state reported). Brazilian pink diamonds have been reported from the Alto Paranaíba province in the state of Minas Gerais; however, the diamonds in alluvial deposits in both Brazil and Venezuela may come from several sources (e.g., Svisero, 1995; Newman et al., 2009; Svisero et al., 2017; Hoover et al., 2018). To the best of our knowledge, only a few diamonds from Brazil have associated published data. Three Brazilian diamonds studied by Kane in 1987 (a 0.54 ct Fancy reddish purple, a 0.59 ct Fancy purple-pink, and a 0.95 ct Fancy purplish red) exhibited "closely spaced red and pink graining and color zonings" and "tatami" features. The photo in that article does not give a clear answer regarding the graining type (wavy band versus discrete lamellae), but the red color appears to be dense, like the Winston Red diamond (again, see figures 7 and 8). Unfortunately, the diamond types were not reported, but the "almost total absorption below 410 nm" suggests they were type Ia. A photo of a "Fancy Red diamond from Brazil" (no carat weight mentioned) in Shigley and Breeding (2013) shows lamellae with a relief effect, such as those from Group 2 diamonds. The current study presents FTIR data for three diamonds reportedly from Minas Gerais, suggesting that alluvial (secondary) deposits in Brazil may produce both Group 1 and Group 2 diamonds. To conclude, narrowing down our geographic origin based on dates of mining operations of Group 1 diamonds suggests that Venezuela or Brazil is the most likely origin of the Winston Red diamond; however, the true origin is still unknown.

CONCLUSIONS

The Winston Red is a magnificent unmodified Fancy red diamond recently gifted to the National Gem and

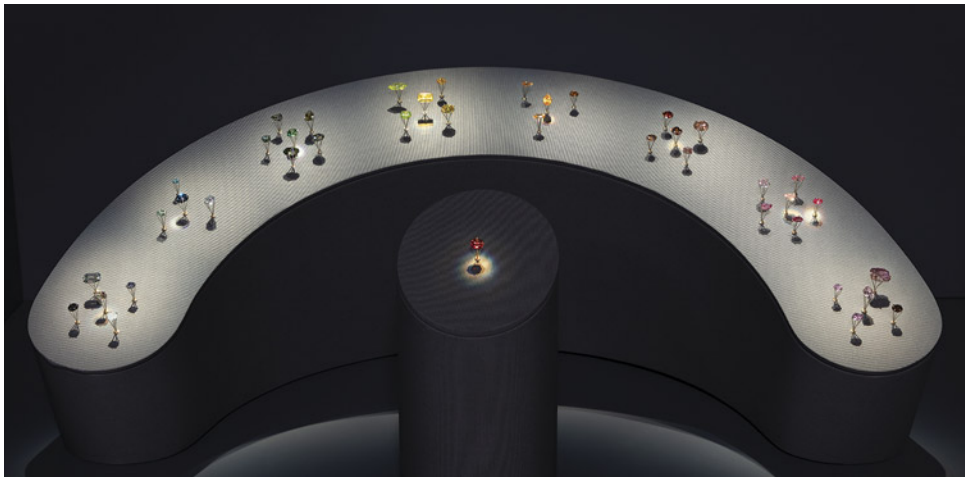

Figure 18. The Winston Red on exhibit with the Winston Fancy Color Diamond Collection in the Winston Gallery of the NMNH. Photo by James Tiller; courtesy of the Smithsonian Institution.

Mineral Collection and has been on public display at the Smithsonian NMNH since April 1, 2025 (figure 18). This first study of the gemstone reveals that the Winston Red diamond is type IaAB, with a low concentration of aggregated nitrogen defects (~7 ppm A-centers and ~76 ppm B-centers, i.e., 92% IaB). Exploring the cause of its iconic red color, a strong 550 nm absorption band is detected, along with absorption from N3 (N_3V^0), H3 (N_2V^0), and H4 ($N_4V_2^0$) centers, in agreement with previous studies of pink and red diamonds. In particular, its uniform red bodycolor is the result of a high density of pink lamellae or grain lines caused by plastic deformation, with intersecting {111}-oriented slip or glide planes aligned along at least three crystallographically equivalent directions. Colorless regions are not observed between lamellae. A cellular network of polygonized dislocations that resemble fish-scale patterns is also observed under CL and PL. Spectral and imaging analyses of the Winston Red suggest that it can be considered a particularly color-saturated example of a Group 1 "pink" diamond (e.g., Gaillou et al., 2010, 2012; Howell et al., 2015). To achieve its red color and dense dislocation networks, the Winston Red diamond likely experienced immense strain under mantle conditions.

To narrow down possible geographic origins of the Winston Red, we explored known Group 1 pink and red diamond deposits that match our historic timeline of the Winston Red diamond (pre-1938). Venezuela or Brazil is the most likely geographic origin; however, too few studies have been conducted on pink or red diamonds from these localities to support a conclusive determination. Hence, the geographic origin of the Winston Red diamond remains unknown.

ABOUT THE AUTHORS

Dr. Gabriela A. Farfan is the Coralyn W. Whitney curator of gems and minerals, and Russell C. Feather II is collection manager for the National Gem Collection, at the Smithsonian Institution, NMNH. Dr. Eloïse Gaillou is director and curator of the Mineralogy Museum of Mines Paris – PSL (Paris School of Mines). Dr. Ulrika F.S. D'Haenens-Johansson is senior manager of diamond research, Stephanie Persaud is a research associate, and Dr. W. Henry Towbin is a postdoctoral research associate, at GIA in New York. Dr. Daniel C. Jones is a research scientist at GIA in New Jersey.

ACKNOWLEDGMENTS

The authors would like to acknowledge Ronald Winston for generously gifting the Winston Red diamond to the National Gem Collection, as well as the many Smithsonian staff who helped facilitate this gift. Many thanks to Rob Wardell and Tim Rose for helping with SEM and CL analyses and to the Department of Mineral Sciences and NMNH staff for accommodating our temporary diamond lab at the NMNH. Wuyi Wang was instrumental in supporting the GIA researchers and making this project happen. Simon Lawson, R.J. Pisani, Mehdi Toosi, and Kevin DeLeon are thanked for developing the photoluminescence spectroscopy device used in this study and rapidly adapting it for mobility. Paola Martinez-Naranjo, Lilia Benjamin, and Paul Johnson are acknowledged for their assistance with the logistical plans for the instrument move. Jon Neal is acknowledged for his helpful insights into the GIA color grading system. Bonnie Zhangluo is thanked for help with the statistical analysis of diamond records at GIA. We also thank Sally Eaton-Magaña, Tom Moses, Simon Lawson, and Andrew Scott for feedback on the manuscript. We thank the archivists at Cartier (especially Libby Dale, Jenny Rourke, César Imbert, Gregory Bishop, and Violette Petit), archivists at Harry Winston, Inc. (especially Angela Hedges, Jennifer Grimes, and Levi Liu), and Francesca Cartier Brickell for their help in uncovering the history of the stone. Gabriela Farfan is supported by the Coralyn Whitney Curator Endowment, and the Department of Mineral Sciences Laboratories are supported by the Coralyn Whitney Laboratory Endowment. W. Henry Towbin is supported by the Richard T. Liddicoat Postdoctoral Research Associate Fellowship at GIA.

REFERENCES

Boyd S.R., Kiflawi I., Woods G.S. (1994) The relationship between infrared absorption and the A defect concentration in diamond. *Philosophical Magazine B*, Vol. 69, No. 6, pp. 1149–1153, http://dx.doi.org/10.1080/01418639408240185

—— (1995) Infrared absorption by the B nitrogen aggregation in diamond. *Philosophical Magazine B*, Vol. 72, No. 3, pp. 351–361, https://doi.org/10.1080/13642819508239089

Breeding C.M., Shigley J.E. (2009) The "type" classification system of diamonds and its importance in gemology. *G&G*, Vol. 45, No. 2, pp. 96–111, http://dx.doi.org/10.5741/GEMS.45.2.96

Brookes E.J., Daniel R.D. (2001) Influence of nitrogen content on the mechanical properties of diamond. In M.H. Nazaré and A.J. Neves, Eds., *Properties, Growth and Applications of Diamond*, Vol. 26, INSPEC, London, pp. 142–148.

Brookes E.J., Greenwood P., Xing G. (1999) The plastic deformation and strain-induced fracture of natural and synthetic diamond. *Diamond and Related Materials*, Vol. 8, No. 8-9, pp. 1536–1539, http://dx.doi.org/10.1016/S0925-9635(99)00080-1

Brookes E.J., Comins J.D., Daniel R.D., Erasmus R.M. (2000) A study of plastic deformation profiles of impressions in diamond. *Diamond and Related Materials*, Vol. 9, No. 3-6, pp. 1115–1119, http://dx.doi.org/10.1016/S0925-9635(99)00203-4

Byrne K.S., Anstie J.D., Chapman J.G., Luiten A.N. (2012) Optically reversible photochromism in natural pink diamond. *Diamond and Related Materials*, Vol. 30, pp. 31–36, http://dx.doi.org/10.1016/j.diamond.2012.09.005

Byrne K.S., Chapman J.G., Luiten A.N. (2014) Photochromic charge transfer processes in natural pink and brown diamonds.

Journal of Physics: Condensed Matter, Vol. 26, No. 3, article no. 035501, http://dx.doi.org/10.1088/0953-8984/26/3/035501
Cartier J. (1934) The Nawanagar Jewels. In R. Wild, *The Biography of Colonel His Highness Shri Sir Ranjitsinhji Vibhaji*. Rich & Cowan Limited, London, pp. 323–326.
Collins A.T. (1982) Colour centers in diamond. *Journal of Gemmology*, Vol. 18, pp. 37–75.
Collins A.T., Woods G.S. (1982) Cathodoluminescence from "giant" platelets, and of the 2•526 eV vibronic system, in type Ia diamonds. *Philosophical Magazine B*, Vol. 45, No. 4, pp. 385–397, http://dx.doi.org/10.1080/01418638208227446
Dean P.J. (1965) Bound excitons and donor-acceptor pairs in natural and synthetic diamond. *Physical Review*, Vol. 139, No. 2A, article no. A588, http://dx.doi.org/10.1103/PhysRev.139.A588
D'Haenens-Johansson U.F.S., Eaton-Magaña S., Towbin W.H., Myagkaya E. (2024) Glowing gems: Fluorescence and phosphorescence of diamonds, colored stones, and pearls. *G&G*, Vol. 60, No. 4, pp. 560–580, http://dx.doi.org/10.5741/GEMS.60.4.560
Deljanin B., Simic D., Zaitsev A., Chapman J., Dobrinets I., Widemann A., Del Re N., Middleton T., Deljanin E., De Stefano A. (2008) Characterization of pink diamonds of different origin: Natural (Argyle, non-Argyle), irradiated and annealed, treated with multi-process, coated and synthetic. *Diamond and Related Materials*, Vol. 17, No. 7-10, pp. 1169–1178, http://dx.doi.org/10.1016/j.diamond.2008.03.014
DeVries R.C. (1975) Plastic deformation and "work-hardening" of diamond. *Materials Research Bulletin*, Vol. 10, No. 11, pp. 1193–1199, http://dx.doi.org/10.1016/0025-5408(75)90026-4
Drukker M. (1971) The red diamond. In A.N. Wilson, Ed., *International Diamond Annual*, Vol. 1, Diamond Annual Ltd., Johannesburg, pp. 140–141.
Eaton-Magaña S., Ardon T., Smit K.V., Breeding C.M., Shigley J.E. (2018) Natural-color pink, purple, red, and brown diamonds: Band of many colors. *G&G*, Vol. 54, No. 4, pp. 352–377, http://dx.doi.org/10.5741/GEMS.54.2.352
Eaton-Magaña S., McElhenny G., Breeding C.M., Ardon T. (2020) Comparison of gemological and spectroscopic features in type IIa and Ia natural pink diamonds. *Diamond and Related Materials*, Vol. 105, article no. 107784, http://dx.doi.org/10.1016/j.diamond.2020.107784
Evans T., Wild R.K. (1965) Plastic bending of diamond plates. *The Philosophical Magazine: A Journal of Theoretical Experimental and Applied Physics*, Vol. 12, No. 117, pp. 479–489, http://dx.doi.org/10.1080/14786436508218894
—— (1966) Plastic deformation of diamond at temperatures below 1800°C. *The Philosophical Magazine: A Journal of Theoretical Experimental and Applied Physics*, Vol. 13, No. 121, pp. 209–210, http://dx.doi.org/10.1080/14786436608211997
Fisher D. (2009) Brown diamonds and high pressure high temperature treatment. *Lithos*, Vol. 112S, pp. 619–624, http://dx.doi.org/10.1016/j.lithos.2009.03.005
Fisher D., Sibley S.J., Kelly C.J. (2009) Brown colour in natural diamond and interaction between the brown related and other colour-inducing defects. *Journal of Physics: Condensed Matter*, Vol. 21, No. 36, article no. 364213, http://dx.doi.org/10.1088/0953-8984/21/36/364213
Fritsch E., Rondeau B., Hainschwang T., Quellier M.-H. (2007) A contribution to the understanding of pink color in diamond: The unique, historical "Grand Condé." *Diamond and Related Materials*, Vol. 16, No. 8. pp. 1471–1474, http://dx.doi.org/10.1016/j.diamond.2006.12.006
Fujita N., Jones R., Öberg S., Briddon P.R. (2009) Large spherical vacancy clusters in diamond – Origin of the brown coloration? *Diamond and Related Materials*, Vol. 18, No. 5-8, pp. 843–845, http://dx.doi.org/10.1016/j.diamond.2008.10.061
Gaal R.A.P. (1977) *The Diamond Dictionary*, 2nd edition, Gemological Institute of America, Santa Monica, CA, 342 pp.
Gaillou E., Post J.E., Bassim N.D., Zaitsev A.M., Rose T., Fries M.D., Stroud R.M., Steele A., Butler J.E. (2010) Spectroscopic and microscopic characterizations of color lamellae in natural pink diamonds. *Diamond and Related Materials*, Vol. 19, No. 10, pp. 1207–1220, http://dx.doi.org/10.1016/j.diamond.2010.06.015
Gaillou E., Post J.E., Rose T., Butler J.E. (2012) Cathodoluminescence of natural, plastically deformed pink diamonds. *Microscopy and Microanalysis*, Vol. 18, No. 6, pp. 1292–1302, http://dx.doi.org/10.1017/S1431927612013542
Gill J.O. (1978) A study of coloured diamonds. *Jewelers' Circular-Keystone*, Vol. 149, No. 6, pp. 83–86.
Green B.L., Collins A.T., Breeding C.M. (2022) Diamond spectroscopy, defect centers, color, and treatments. *Reviews in Mineralogy and Geochemistry*, Vol. 88, No. 1, pp. 637–688, http://dx.doi.org/10.2138/rmg.2022.88.12
Goss J.P., Briddon P.R., Hill V., Jones R., Rayson M.J. (2014) Identification of the structure of the 3107 cm^{-1} H-related defect in diamond. *Journal of Physics: Condensed Matter*, Vol. 26, No. 14, article no. 145801, http://dx.doi.org/10.1088/0953-8984/26/14/145801
Guagliardo P., Byrne K., Chapman J., Sudarshan K., Samarin S., Williams J. (2013) Positron annihilation and optical studies of natural brown type I diamonds. *Diamond and Related Materials*, Vol. 37, pp. 37–40, http://dx.doi.org/10.1016/j.diamond.2013.04.011
Harlow G.E. (1998) *The Nature of Diamonds*. Eds: American Museum of Natural History, George E. Harlow. Cambridge University Press, 278 pp.
Harris J.W., Smit K.V., Fedortchouk Y., Moore M. (2022) Morphology of monocrystalline diamond and its inclusions. *Reviews in Mineralogy and Geochemistry*, Vol. 88, No. 1, pp. 119–166, http://dx.doi.org/10.2138/rmg.2022.88.02
Hoover D.B., Karfunkel J., Walde D., Moraes R.A.V., Michelfelder G., Renger F.E., Ribeiro L.C.B., Krambrock K., Klock C.F. (2018) The Alto Paranaíba region, Brazil: A continuing source for pink diamonds? *Australian Gemmologist*, Vol. 26, No. 9-10, pp. 196–204.
Howell D., Fisher D., Piazolo S., Griffin W.L., Sibley S.J. (2015) Pink color in type I diamonds: Is deformation twinning the cause? *American Mineralogist*, Vol. 100, No. 7, pp. 1518–1527, http://dx.doi.org/10.2138/am-2015-5044
Iakoubovskii K., Adriaenssens G.J. (2002) Optical characterization of natural Argyle diamonds. *Diamond and Related Materials*, Vol. 11, No. 1, pp. 125–131, http://dx.doi.org/10.1016/S0925-9635(01)00533-7
Jones R. (2009) Dislocations, vacancies and the brown colour of CVD and natural diamond. *Diamond and Related Materials*, Vol. 18, No. 5-8, pp. 820–826, http://dx.doi.org/10.1016/j.diamond.2008.11.027
Kaminsky F.V., Zakharchenko O.D., Griffin W.L., Channer D.M. DeR., Khachatryan-Blinova G.K. (2000) Diamond from the Guaniamo area, Venezuela. *Canadian Mineralogist*, Vol. 38, No. 6, pp. 1347–1370, http://dx.doi.org/10.2113/gscanmin.38.6.1347
Kanda H., Ahmadjan A., Kitawaki H. (2005) Change in cathodoluminescence spectra and images of type II high-pressure synthetic diamond produced with high pressure and temperature treatment. *Diamond and Related Materials*, Vol. 14, No. 11–12, pp. 1928–1931, https://doi.org/10.1016/j.diamond.2005.08.015
Keswani R. (2004) *Shinde Jewels*. Assouline, New York.
King J.M., Moses T.M., Shigley J.E., Liu Y. (1994) Color grading of colored diamonds in the GIA Gem Trade Laboratory. *G&G*, Vol. 30, No. 4, pp. 220–242, http://dx.doi.org/10.5741/GEMS.30.4.220
King J.M., Shigley J.E., Guhin S.S., Gelb T.H., Hall M. (2002) Characterization and grading of natural-color pink diamonds. *G&G*, Vol. 38, No. 2, pp. 128–147, http://dx.doi.org/10.5741/GEMS.38.2.128
King J.M., Shigley J.E. (2003) An important exhibition of seven rare gem diamonds. *G&G*, Vol. 39, No. 2, pp. 136–143, http://dx.doi.org/10.5741/GEMS.39.2.136
King J.M., Shigley J.E., Jannucci C. (2014) Exceptional pink to red

diamonds: A celebration of the 30th Argyle Diamond Tender. *G&G*, Vol. 50, No. 4, pp. 268–279, http://dx.doi.org/10.5741/GEMS.50.4.268
Kane R.E. (1987) Three notable fancy-color diamonds: Purplish red, purple-pink, and reddish purple. *G&G*, Vol. 23, No. 2, pp. 90–95, http://dx.doi.org/10.5741/GEMS.23.2.90
Kunz G.F. (1926) Precious Stones. In G.A. Roush, Ed., *The Mineral Industry - Its Statistics, Technology, and Trade during 1925*. McGraw Hill, New York, NY, 906 pp.
Laidlaw F.H.J., Diggle P.L., Breeze B.G., Dale M.W., Fisher D., Beanland R. (2021) Spatial distribution of defects in a plastically deformed natural brown diamond. *Diamond and Related Materials*, Vol. 117, article no. 108465, http://dx.doi.org/10.1016/j.diamond.2021.108465
Luo Y., Breeding C.M. (2013) Fluorescence produced by optical defects in diamond: Measurement, characterization, and challenges. *G&G*, Vol. 49, No. 2, pp. 82–97, http://dx.doi.org/10.5741/GEMS.49.2.82
Machado W.G., Moore M., Woods G.S. (1985) On the dodecahedral growth of coated diamonds. *Journal of Crystal Growth*, Vol. 71, No. 3, pp. 718–727, http://dx.doi.org/10.1016/0022-0248(85)90382-3
Mäki J.-M., Tuomisto F., Kelly C.J., Fisher D., Martineau P.M. (2009) Properties of optically active vacancy clusters in type IIa diamond. *Journal of Physics: Condensed Matter*, Vol. 21, article number 364216, http://dx.doi.org/10.1088/0953-8984/21/36/364216
Massi L., Fritsch E., Collins A.T., Hainschwang T., Notari F. (2005) The "amber centres" and their relation to the brown colour in diamond. *Diamond and Related Materials*, Vol. 14, No. 10, pp. 1623–1629, http://dx.doi.org/10.1016/j.diamond.2005.05.003
Mineeva R.M., Speransky A.V., Titkov S.V., Zudin N.G. (2007) The ordered creation of paramagnetic defects at plastic deformation of natural diamonds. *Physics and Chemistry of Minerals*, Vol. 34, pp. 53–58, http://dx.doi.org/10.1007/s00269-006-0127-5
Mineeva R.M., Titkov, S.V., Speransky, A.V. (2009) Structural defects in natural plastically deformed diamonds: Evidence from EPR spectroscopy. *Geology of Ore Deposits*, Vol. 51, pp. 233–242, http://dx.doi.org/10.1134/S1075701509030052
Monnickendam A. (1955) *The Magic of Diamonds*. Hamond, Hamond and Company, London, 191 pp.
Newman J.A., de Newman Carvalho D.T., Gandini A.L., Gomes N.S., Rojas A.J. (2009) Caracterizacion mineralogica del diamante de los placeres aluvionales del Rio Icaburu, Santa Elena de Uairen, Estado Bolivar, Venezuela. *Revista de la Asociacion Geologica Argentina*, Vol. 64, No. 3, pp. 472–480.
Nimis P. (2022) Pressure and temperature data for diamonds. *Reviews in Mineralogy and Geochemistry*, Vol. 88, No. 1, pp. 533–565, http://dx.doi.org/10.2138/rmg.2022.88.10
Orlov Y.L. (1977) *The Mineralogy of the Diamond*. New York: Wiley & Sons, 248 pp.
Palik E.D. (1985) *Handbook of Optical Constants of Solids*. Academic Press, London.
Rolandi V., Brajkovic A., Adamo I., Fontana I. (2008) Argyle type Ia pink diamonds. Gemmological properties, FTIR, UV-Vis and CL features. *Australian Gemmologist*, Vol. 23, No. 5, pp. 194–203.
Ruan J., Kobashi K., Choyke W.J. (1992) On the "band-A" emission and boron related luminescence in diamond. *Applied Physics Letters*, Vol. 60, No. 25, pp. 3138–3140, http://dx.doi.org/10.1063/1.106748
Schneider G.I.C. (2020) Marine diamond mining in the Benguela Current Large Marine Ecosystem: The case of Namibia. *Environmental Development*, Vol. 36, article no. 100579, http://dx.doi.org/10.1016/j.envdev.2020.100579
Schoor M., Boulliard J.C., Gaillou E., Duparc O.H., Estève I., Baptiste B., Rondeau B., Fritsch E. (2016) Plastic deformation in natural diamonds: Rose channels associated to mechanical twinning. *Diamond and Related Materials*, Vol. 66, pp. 102–106, https://doi.org/10.1016/j.diamond.2016.04.004
Shepherd G.F. (1934) Largest ruby-red diamond. *G&G*, Vol. 1, No. 6, p. 172.
Shigley J.E., Fritsch E. (1993) A notable red-brown diamond. *Journal of Gemmology*, Vol. 23. No. 5, pp. 259–266.
Shigley J.E., Chapman J., Ellison R.K. (2001) Discovery and mining of the Argyle diamond deposit, Australia. *G&G*, Vol. 37, No. 1, pp. 26–41, http://dx.doi.org/10.5741/GEMS.37.1.26
Shigley J.E., Breeding C.M. (2013) Optical defects in diamond: A quick reference chart. *G&G*, Vol. 49, No. 2, pp. 107–111, http://dx.doi.org/10.5741/GEMS.49.2.107
Smith E.M., Helmstaedt H.H., Flemming R.L. (2010) Survival of the brown color in diamond during storage in the subcontinental lithospheric mantle. *Canadian Mineralogist*, Vol. 48, No. 3, pp. 571–582, http://dx.doi.org/10.3749/canmin.48.3.571
Smith E.M., Smit K.V., Shirey S.B. (2022) Methods and challenges of establishing the geographic origin of diamonds. *G&G*, Vol. 58, No. 3, pp. 270–288, http://dx.doi.org/10.5741/GEMS.58.3.270
Smith E.M. (2023) Plastic deformation: How and why are most diamonds slightly distorted? *G&G*, Vol. 59, No. 1, pp. 94–100.
Speich L., Kohn S.C., Wirth R., Bulanova G.P., Smith C.B. (2017) The relationship between platelet size and the B′ infrared peak of natural diamonds revisited. *Lithos*, Vol. 278-281, pp. 419–426, http://dx.doi.org/10.1016/j.lithos.2017.02.010
Spink M. (2018) Indian passion. In *The Cartier Collection: Jewelry, Vol. 1*, Flammarion, Paris, pp. 256–276.
Stachel T., Harris J.W. (2008) The origin of cratonic diamonds – Constraints from mineral inclusions. *Ore Geology Reviews*, Vol. 34, No. 1-2, pp. 5–32, http://dx.doi.org/10.1016/j.oregeorev.2007.05.002
Sumida N., Lang A.R. (1981) Cathodoluminescence evidence of dislocation interactions in diamond. *Philosophical Magazine A*, Vol. 43, No. 5, pp. 1277–1287, http://dx.doi.org/10.1080/01418618108236156
Svisero D.P. (1995) Distribution and origin of diamonds in Brazil: An overview. *Journal of Geodynamics*, Vol. 20, No. 4, pp. 493–514, http://dx.doi.org/10.1016/0264-3707(95)00017-4
Svisero D.P., Shigley J.E., Weldon R. (2017) Brazilian diamonds: A historical and recent perspective. *G&G*, Vol. 53, No. 1, pp. 2–33, http://dx.doi.org/10.5741/GEMS.53.1.2
Thomaz M.F., Davies G. (1978) The decay time of N3 luminescence in natural diamond. *Proceedings of the Royal Society of London, Series A*, Vol. 362, No. 1710, pp. 405–419, http://dx.doi.org/10.1098/rspa.1978.0141
Titkov S.V., Krivovichev S.V., Organova N.I. (2012) Plastic deformation of natural diamonds by twinning: Evidence from X-ray diffraction studies. *Mineralogical Magazine*, Vol. 76, No. 1, pp. 143–149, http://dx.doi.org/10.1180/minmag.2012.076.1.143
Welbourn C.M., Cooper M., Spear P.M. (1996) De Beers natural versus synthetic diamond verification instruments. *G&G*, Vol. 32, No. 3, pp. 156–169, http://dx.doi.org/10.5741/GEMS.32.3.156
Wild R.K., Evans T., Thomson J.J., Lang A.R. (1967) Birefringence, x-ray topography and electron microscope examination of the plastic deformation of diamond. *Philosophical Magazine*, Vol. 15, No. 134, pp. 267–279, http://dx.doi.org/10.1080/14786436708227700
Wilhelm K.F.A. (1860) *Catalogue de Brillants et Autres Pierres Precieuses de Son Altesse Monseigneur le duc Soverain de Brunswick-Lunebourg*. chez Chauvet, Bijoutier, Paris, 282 pp., https://archive.org/details/CatalogueDeBrillantsEtAutresPierresPrecieusesDeSonAltesseMonseigneur/mode/2up
Wilson W.E. (2014) Red diamond. *Mineralogical Record*, Vol. 45, No. 2, pp. 201–214.
Woods G.S. (1986) Platelets and the infrared absorption of type Ia diamonds. *Proceedings of the Royal Society of London, Series A*, Vol. 407, No. 1832, pp. 219–238, http://dx.doi.org/10.1098/rspa.1986.0094